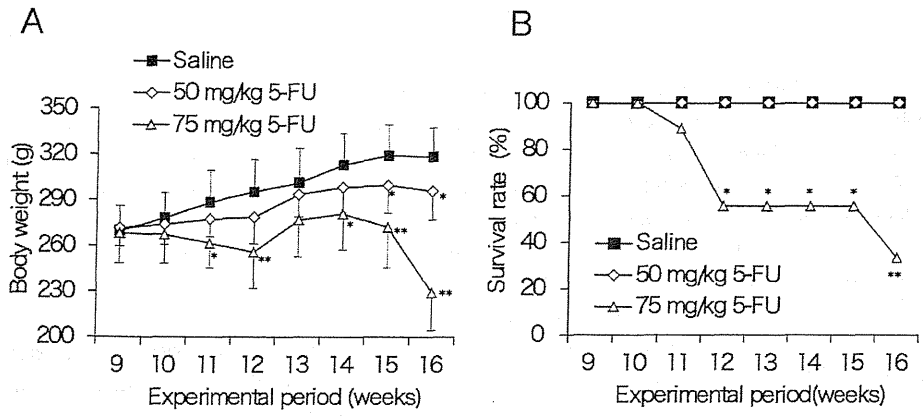

Figure 3 Toxicity of 5-FU in AOM/DSS treated KAD rats. Average body weight (**A**) and survival rate (**B**) of the control, 50 mg/kg and 75 mg/kg 5-FU treated groups. *$p < 0.05$, **$p < 0.001$.

significant elevation of cleaved caspase-3 positive rate in the adenocarcinomas in Group 1 (Figure 6). These results suggest that the 5-FU treatment suppressed cell proliferation and induced apoptosis and thereby inhibited adenocarcinoma development.

Discussion

Carcinogenic process is complex. Tumor development proceeds via a multi-step process, in which a succession of genetic changes, each conferring one or another type of growth advantage, leads to the progressive conversion of normal cells into cancer cells. Moreover, extent of cell transformation depends on the genetic predisposition and environmental factors [13]. Thus, to obtain cancerous lesions effectively, it is necessary to use a synergy effect of genetic and environmental factors. Our carcinogenic system with KAD rats employs such synergy effect of *Apc*-mutation, chemical carcinogen exposure, and tissue inflammation.

In ideal chemotherapeutic bioassay systems, the number and volume of tumors should be evaluated as the indicator of anti-tumor drug efficacy. Therefore, it is indispensable to be able to strictly set the size of the experimental and control groups, among which the number and volume of tumors should not differ significantly. To this end, we carried out endoscopic observations in the colons of AOM/DSS-treated KAD rats, and divided animals into groups on the basis of the number of colon tumors. Since the rat has a suitable body size for handling, we could easily manipulate the endoscope and correctly count the number of tumors. At week 8 we found colon tumors with a 100% incidence in AOM/DSS-treated KAD rats. The rats developed one to four tumors. On the basis of the number of tumors, we could set the experimental and control groups, because

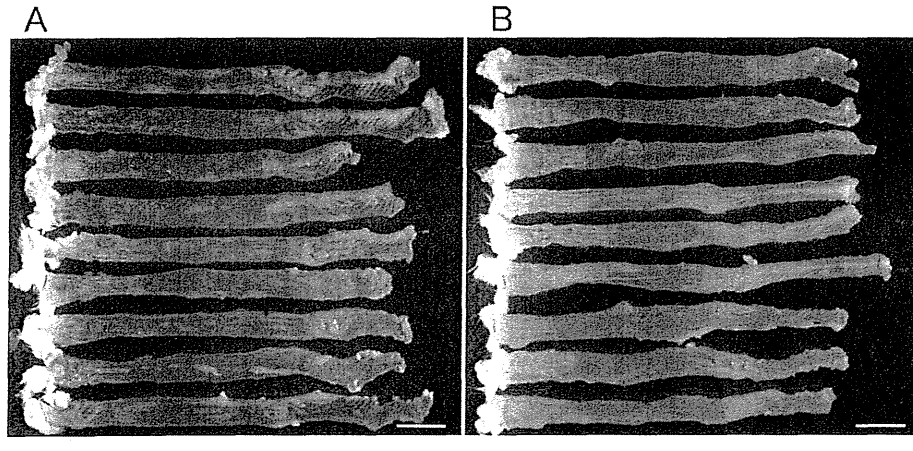

Figure 4 Macroscopic view of large bowel. Macroscopic view of large bowel of KAD rats that were not given 5-FU (**A**) and that were given 50 mg/kg 5-FU (**B**). Colon tumors that developed in both groups were mainly distributed in the rectum and distal colon, which was assumed to be within 8 cm from the anus. No tumors were observed in the proximal colon. Left side: anus. Right side: cecum. Bar: 2 cm.

Table 1 Effects of 5-FU on the development of colon tumors in the KAD rat

Treatment	No. of rats	Macroscopic observation		Microscopic observation			
		Multiplicity	Volume (mm^3)[1]	Multiplicity			Volume (mm^3)[2]
				adenomas	adenocarcinomas	total	adenocarcinoma
Saline	9	5.56 ± 3.43	106.34 ± 68.92	3.11 ± 2.52	3.22 ± 2.77	6.33 ± 4.87	63.85 ± 51.06
50 mg/kg 5-FU	9	6.33 ± 3.04	77.28 ± 57.23	3.78 ± 1.79	2.33 ± 1.94	6.11 ± 2.37	34.40 ± 31.26 [3]

[1]Tumor volume was determined by the formula $V = a \times b^2/2$ (V: volume. a: the largest superficial diameter and b: the smallest superficial diameter).
[2]Volumes of adenomas were too small to calculate.
[3]Adenocarcinoma volumes observed in the 5-FU-treated KAD rats were significantly reduced as compared with those of non-treated rats ($p < 0.02$).

the number of tumors observed by the endoscopy is correlated to the volume of tumors obtained by the microscopy at week 8. We, therefore, recommend counting the number of tumors using endoscopic observation before dividing the rats into groups.

It is important to identify biomarkers that are used to predict efficacy and safety of anti-tumor drugs. Rats can be subjected to the sequential sampling of bloods. The amounts of bloods or urines are enough to be examined. Moreover, drug kinetics can be monitored by *in vivo* imaging [14]. Thus, the chemotherapeutic bioassay with the KAD rats is a candidate system to explore the biomarkers.

5-FU is a pyrimidine analog and when incorporated into DNA inhibits the cell's ability to synthesize DNA. Eventually 5-FU induces cell cycle arrest and apoptosis, mainly in cells with high proliferative activity such as cancer cells [15]. Side effects of 5-FU, such as diarrhea and weight loss, are problematic in performing chemotherapeutic tests with animal models. Thus, it is important to determine the maximum tolerated dose (MTD) that does not produce profound weight loss, and that causes no drug-related lethality. Usually the MTD of 5-FU in rats ranges from 25 to 100 mg/kg, depending on the 5-FU administration schedules [16]. In the current study, we found that the MTD was 50 mg/kg of 5-FU when administered to tumor-bearing KAD rats by i.v. injection. Although the MTD should be determined using different administration schedules and routes, the MTD that we determined in the present study can be a helpful guide in setting doses of anti-cancer drugs in further chemotherapeutic tests with KAD rats.

In our study, the treatment of tumor-bearing KAD rats with 5-FU failed to reduce the multiplicity of adenoma or adenocarcinoma. However, the treatment significantly reduced adenocarcinoma tumor volume and cell proliferation as well as increased adenocarcinoma apoptosis, which was consistent with the mode of action of the 5-FU [15]. Treatment response assessed in terms of

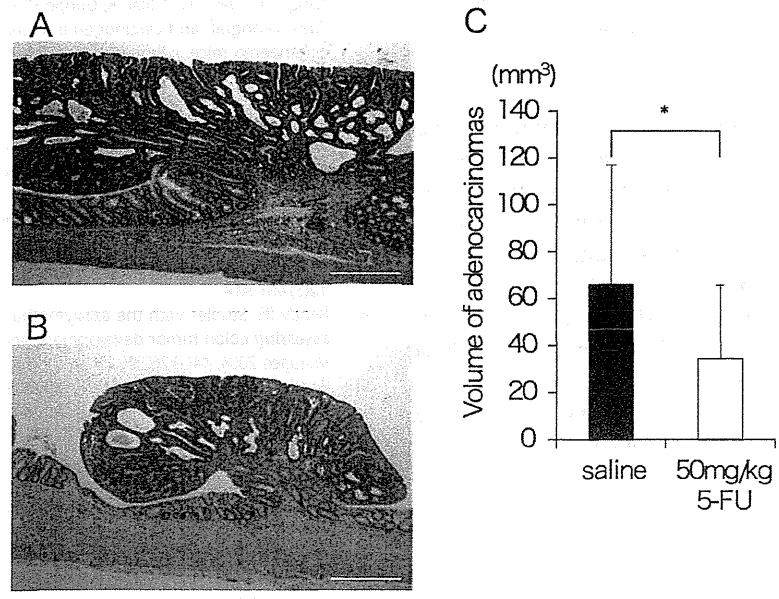

Figure 5 Histopathological analysis of colonic adenocarcinomas. Colonic adenocarcinoma developed in KAD rats that were not given 5-FU (**A**) and that were given 50 mg/kg 5-FU (**B**). Most of the adenocarcinomas in KAD rats that received 50 mg/kg 5-FU were smaller than those in the control group (hematoxylin and eosin stain). Bar: 500 □m. (**C**) Average volume of adenocarcinoma tumors grown in KAD rats that were given saline or 5-FU (50 mg/kg). The mean volume of adenocarcinoma tumors in the 5-FU-treated rats were significantly smaller than those in the non-treated rats. *: $p < 0.02$.

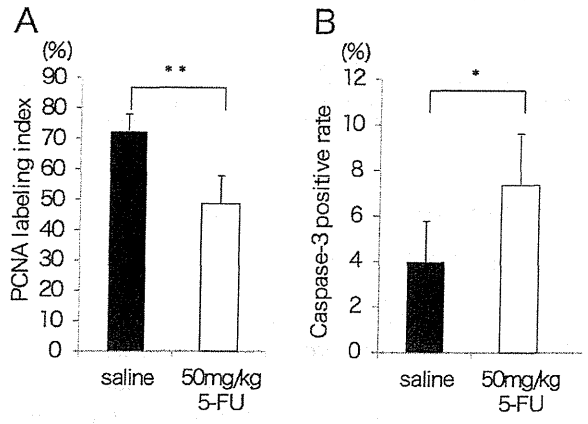

Figure 6 Cell proliferation and apoptosis in adenocarcinomas of the 5-FU treated KAD rats. (**A**) The PCNA labeling index was significantly lower in the 5-FU treated KAD rats (50 mg/kg) than that in the control KAD rats, indicating significant decrease in cell proliferation in the adenocarcinomas. **: $p < 0.001$. (**B**) The cleaved caspase-3 positive rate was significantly higher in the 5-FU treated KAD rats (50 mg/kg) than that in the control KAD rats, indicating significant increase in apoptosis in the adenocarcinomas. *: $p < 0.02$.

change in tumor size after 5-FU administration in the present study amounted to a 30% reduction, which was similar to the response rate of 5-FU as a single agent seen in human cancers, including CRC [17]. These findings indicated that the response of tumors in AOM/DSS-treated KAD rats to 5-FU treatment was similar to human CRC, and supported the view that this should be a useful bioassay system for employment in further chemotherapeutic studies.

Conclusions

In the present study we established a chemotherapeutic bioassay system for CRC using KAD rats. In this system, we could set the experimental groups on the basis of the number of tumors detected by endoscopic examination. After 5-FU administration rat colon tumors induced by AOM/DSS treatments showed a similar response, in terms of percentage reduction in size and cell proliferation and percentage elevation in apoptosis, to those reported in clinical CRC studies. Thus, we expect that this system could effectively promote the development of new anti-tumor drugs and regimens for human CRC.

Additional files

Additional file 1: Table S1. Number and total volume of tumors found in KAD rats at week 8.

Additional file 2: Figure S1. The correlation of total volume of tumors with the numbers of polypoid lesions observed by endoscopy at Week8. Regression formula was made with Excel software package (Microsoft). Vertical axis was shown in logarithmic scale.

Competing interests

The authors declare that they have no competing interests.

Authors' contributions

KY and TK conceived the study and designed the experiments. KY, TH, YN and KH performed the experiments. TT performed the histopathological analysis. KY, TK and TT wrote the manuscript. TS revised the manuscript. All authors have read and approved the final manuscript.

Acknowledgments

This work was supported in part by a Grant-in-Aid for Cancer Research from the Ministry of Health, Labour and Welfare (to TK), and Grants-in-Aid for Scientific Research from the Japan Society for the Promotion of Science (21300153 to TK and 0233639 to KY). The KAD (F344-*Apc*^{m1Kyo}) rat has been deposited in the National BioResource Project-Rat in Japan and is available from the Project (http://www.anim.med.kyoto-u.ac.jp/nbr).

Author details

[1]Institute of Laboratory Animals, Graduate School of Medicine, Kyoto University, Yoshidakonoe-cho, Sakyo-ku, Kyoto 606-8501, Japan. [2]Sunplanet Co., Ltd, 4388 Makita, Kamiishizu, Ogaki 503-1602, Japan. [3]Cancer Research and Prevention, The Tohkai Cytopathology Institute, 4-33 Minami-Uzura, Gifu 500-8285, Japan.

Received: 24 April 2012 Accepted: 26 September 2012
Published: 3 October 2012

References

1. Blumenthal RD, Osorio L, Hayes MK, Horak ID, Hansen HJ, Goldenberg DM: Carcinoembryonic antigen antibody inhibits lung metastasis and augments chemotherapy in a human colonic carcinoma xenograft. *Cancer Immunol Immunother* 2005, 54(4):315□327.
2. Corpet DE, Pierre F: Point: From animal models to prevention of colon cancer. Systematic review of chemoprevention in min mice and choice of the model system. *Cancer Epidemiol Biomarkers Prev* 2003, 12(5):391□400.
3. Williams KJ, Telfer BA, Stratford IJ, Wedge SR: ZD1839 (Iressa), a specific oral epidermal growth factor receptor-tyrosine kinase inhibitor, potentiates radiotherapy in a human colorectal cancer xenograft model. *Br J Cancer* 2002, 86(7):1157□1161.
4. Ding Y, Cravero JD, Adrian K, Grippo P: Modeling pancreatic cancer *in vivo*: from xenograft and carcinogen-induced systems to genetically engineered mice. *Pancreas* 2010, 39(3):283□292.
5. Voskoglou-Nomikos T, Pater JL, Seymour L: Clinical predictive value of the *in vitro* cell line, human xenograft, and mouse allograft preclinical cancer models. *Clin Cancer Res* 2003, 9(11):4227□4239.
6. Femia AP, Caderni G: Rodent models of colon carcinogenesis for the study of chemopreventive activity of natural products. *Planta Med* 2008, 74(13):1602□1607.
7. Bruce WR: Counterpoint: From animal models to prevention of colon cancer. Criteria for proceeding from preclinical studies and choice of models for prevention studies. *Cancer Epidemiol Biomarkers Prev* 2003, 12(5):401□404.
8. Reddy BS: Studies with the azoxymethane-rat preclinical model for assessing colon tumor development and chemoprevention. *Environ Mol Mutagen* 2004, 44(1):26□35.
9. Reddy BS, Maeura Y: Tumor promotion by dietary fat in azoxymethane-induced colon carcinogenesis in female F344 rats: influence of amount and source of dietary fat. *J Natl Cancer Inst* 1984, 72(3):745□750.
10. Tanaka T, Kohno H, Suzuki R, Yamada Y, Sugie S, Mori H: A novel inflammation-related mouse colon carcinogenesis model induced by azoxymethane and dextran sodium sulfate. *Cancer Sci* 2003, 94(11):965□973.
11. Yoshimi K, Tanaka T, Takizawa A, Kato M, Hirabayashi M, Mashimo T, Serikawa T, Kuramoto T: Enhanced colitis-associated colon carcinogenesis in a novel Apc mutant rat. *Cancer Sci* 2009, 100(11):2022□2027.
12. Carlsson G, Gullberg B, Hafstrom L: Estimation of liver tumor volume using different formulas - an experimental study in rats. *J Cancer Res Clin Oncol* 1983, 105(1):20□23.
13. Hanahan D, Weinberg RA: The hallmarks of cancer. *Cell* 2000, 100(1):57□70.
14. Ogawa K, Mukai T, Kawai K, Takamura N, Hanaoka H, Hashimoto K, Shiba K, Mori H, Saji H: Usefulness of competitive inhibitors of protein binding for

improving the pharmacokinetics of 186Re-MAG3-conjugated bisphosphonate (186Re-MAG3-HBP), an agent for treatment of painful bone metastases. *Eur J Nucl Med Mol Imaging* 2009, 36(1):115□121.
15. Thomas DM, Zalcberg JR: 5-fluorouracil: a pharmacological paradigm in the use of cytotoxics. *Clin Exp Pharmacol Physiol* 1998, 25(11):887□895.
16. Cao S, Rustum YM: Synergistic antitumor activity of irinotecan in combination with 5-fluorouracil in rats bearing advanced colorectal cancer: role of drug sequence and dose. *Cancer Res* 2000, 60(14):3717□3721.
17. Salonga D, Danenberg KD, Johnson M, Metzger R, Groshen S, Tsao-Wei DD, Lenz HJ, Leichman CG, Leichman L, Diasio RB, *et al*: Colorectal tumors responding to 5-fluorouracil have low gene expression levels of dihydropyrimidine dehydrogenase, thymidylate synthase, and thymidine phosphorylase. *Clin Cancer Res* 2000, 6(4):1322□1327.

doi:10.1186/1471-2407-12-448
Cite this article as: Yoshimi *et al.*: Use of a chemically induced-colon carcinogenesis-prone *Apc*-mutant rat in a chemotherapeutic bioassay. *BMC Cancer* 2012 12:448.

Carcinogenesis vol.33 no.12 pp.2499–2506, 2012
doi:10.1093/carcin/bgs303
Advance Access publication October 2, 2012

Preventive effects of branched-chain amino acid supplementation on the spontaneous development of hepatic preneoplastic lesions in C57BL/KsJ-*db/db* obese mice

Daishi Terakura[1], Masahito Shimizu[1,*], Junpei Iwasa[1], Atsushi Baba[1], Takahiro Kochi[1], Tomohiko Ohno[1], Masaya Kubota[1], Yohei Shirakami[1], Makoto Shiraki[1], Koji Takai[1], Hisashi Tsurumi[1], Takuji Tanaka[2] and Hisataka Moriwaki[1]

[1]Department of Gastroenterology, Gifu University Graduate School of Medicine, Gifu 501–1194, Japan and [2]The Tohkai Cytopathology Institute: Cancer Research and Prevention (TCI-CaRP), Gifu 500–8285, Japan

*To whom correspondence should be addressed. Masahito Shimizu, Department of Gastroenterology, Gifu University Graduate School of Medicine, 1-1 Yanagido, Gifu 501–1194, Japan. Tel: +81 58 230 6313; Fax: +81 58 230 6310;
Email: shimim-gif@umin.ac.jp

Obesity and its associated disorders, such as non-alcoholic steatohepatitis, increase the risk of hepatocellular carcinoma. Branched-chain amino acids (BCAA), which improve protein malnutrition in patients with liver cirrhosis, reduce the risk of hepatocellular carcinoma in these patients with obesity. In the present study, the effects of BCAA supplementation on the spontaneous development of hepatic premalignant lesions, foci of cellular alteration, in *db/db* obese mice were examined. Male *db/db* mice were given a basal diet containing 3.0% of either BCAA or casein, a nitrogen-content-matched control of BCAA, for 36 weeks. On killing the mice, supplementation with BCAA significantly inhibited the development of foci of cellular alteration when compared with casein supplementation by inhibiting cell proliferation, but inducing apoptosis. BCAA supplementation increased the expression levels of peroxisome proliferator-activated receptor-γ, $p21^{CIP1}$ and $p27^{KIP1}$ messenger RNA and decreased the levels of c-*fos* and cyclin D1 mRNA in the liver. BCAA supplementation also reduced both the amount of hepatic triglyceride accumulation and the expression of interleukin (IL)-6, IL-1β, IL-18 and tumor necrosis factor-α mRNA in the liver. Increased macrophage infiltration was inhibited and the expression of IL-6, TNF-α, and monocyte chemoattractant protein-1 mRNA in the white adipose tissue were each decreased by BCAA supplementation. BCAA supplementation also reduced adipocyte size while increasing the expression of peroxisome proliferator-activated receptor-α, peroxisome proliferator-activated receptor-γ and adiponectin mRNA in the white adipose tissue compared with casein supplementation. These findings indicate that BCAA supplementation inhibits the early phase of obesity-related liver tumorigenesis by attenuating chronic inflammation in both the liver and white adipose tissue. BCAA supplementation may be useful in the chemoprevention of liver tumorigenesis in obese individuals.

Introduction

Obesity is a serious health problem worldwide since it often causes a number of medical disorders, including metabolic syndrome and type 2 diabetes mellitus. Recent evidence also indicates that obesity and its related metabolic abnormalities are associated with an increased risk of developing hepatocellular carcinoma (HCC (1–5)). Non-alcoholi fatty liver disease (NAFLD) is a hepatic manifestation of metaboli syndrome and a subset of patients with this disease can progress t non-alcoholic steatohepatitis (NASH), which involves the risk o developing chronic hepatitis, cirrhosis and HCC (6–8). Obesity an diabetes mellitus have been shown to increase the risk of develop ing HCC also in patients with viral hepatitis (3,5). A state of chroni inflammation caused by insulin resistance and hepatic steatosis is con sidered to play a critical role in the development of HCC in severa obesity-related pathophysiological conditions (2,6–10). Therefore obese patients, especially those with complications of NASH o chronic viral hepatitis, are at high risk for developing HCC, and tar geting chronic inflammation might be an effective strategy for pre venting obesity-related liver carcinogenesis (11).

Branched-chain amino acids (BCAA), which are a group of three essential amino acids comprising valine, leucine and isoleucine, are used clinically to improve protein malnutrition in patients with liver cirrhosis (12,13). Oral supplementation with BCAA prevents progressive hepatic failure and improves event-free survival in patients with chronic liver diseases (14,15). Moreover, a multicenter, randomized controlled trial has reported that long-term oral BCAA supplementation reduced the risk of developing HCC in patients with chronic viral hepatitis; however, the effect was evident only in the patients who are obese (3). The results seen in that clinical trial are considered to be associated with the improvement of insulin resistance achieved by BCAA supplementation (13,16). In fact, BCAA supplementation inhibited the development of carcinogen-induced liver and colorectal carcinogenesis in obese mice by improving insulin resistance (17,18). Treatment with BCAA also suppressed insulin-induced proliferation of HCC cells by antagonizing the anti-apoptotic function of insulin (19).

In addition to improving protein malnutrition and glucose metabolism, BCAA supplementation has been reported to reduce lipid deposition in the liver in recent rodent studies (17,20). Supplementation with BCAA also retarded excess weight gain and reduced epididymal white adipose tissue (WAT) weight in mice that fed a high-fat diet (20). Because chronic low-grade systemic inflammation produced by excess lipid storage in WAT and liver is involved in both the development of NASH and the obesity-related liver tumorigenesis (2,6–10), BCAA supplementation may prevent the development of liver neoplasms in obese mice by reducing excess fat accumulation in WAT and by improving liver steatosis, thereby attenuating inflammation in these organs.

The spontaneous development of hepatic preneoplastic lesions, foci of cellular alteration (FCA), have been previously reported to be enhanced in obese and diabetic C57BL/KsJ-*db/db* (*db/db*) mice, when compared with C57B6 or C57BL/KsJ-+/+ mice, genetic controls for *db/db* mice (17). In the present study, we examined the effects of BCAA supplementation on the spontaneous development of FCA in *db/db* mice while focusing on the attenuation of inflammation in both the liver and the WAT. In addition, we investigated whether BCAA supplementation alters adipocyte size and the expression of peroxisome proliferator-activated receptor (PPAR)-α, PPAR-γ and adiponectin, which are key regulators of inflammatory signaling in obese adipose tissue (21–25), in the WAT of *db/db* mice.

Abbreviations: BCAA, branched-chain amino acids; FCA, foci of cellular alteration; HCC, hepatocellular carcinoma; H&E, hematoxylin and eosin; IL: interleukin; NAFLD, non-alcoholic fatty liver disease; NASH, non-alcoholic steatohepatitis; PCNA, proliferating cell nuclear antigen; PPAR, peroxisome proliferator-activated receptor; RT–PCR, reverse transcription–PCR; SEM, standard error mean; TNF-α, tumor necrosis factor-α; WAT, white adipose tissue.

Materials and methods

Mice and diets

Male *db/db* mice (4 weeks old) were obtained from Japan SLC (Shizuoka, Japan) and humanely maintained at Gifu University Life Science Research Center in accordance with Institutional Animal Care Guidelines. BCAA and casein were obtained from Ajinomoto (Tokyo, Japan). The BCAA composition (2:1:1.2 = leucine:isoleucine:valine) was set at the clinical dosage used for the treatment of decompensated liver cirrhosis in Japan (3,14).

Experimental procedure

The experimental protocol was approved by the Institutional Committee of Animal Experiments of Gifu University. At 5 weeks of age, a total of 10 *db/db* mice were divided into two groups. The mice in Group 2 ($n = 5$) were given a basal diet (CRF-1, Oriental Yeast, Tokyo, Japan) supplemented with 3.0% BCAA (w/w) through the end of the experiment, whereas the mice in Group 1 ($n = 5$) were given a basal diet supplemented with 3.0% casein (w/w) that served as a nitrogen-content-matched control for the BCAA-treated group. At 41 weeks of age (after 36 weeks of supplementation with the experimental diet), all of the mice were killed using CO_2 asphyxiation and the development of FCA was analyzed.

Histopathology and measurement of adipocyte size

Maximum sagittal sections of each liver lobe (six sublobes) and WAT obtained from the periorchis were used for histological examination. The tissue specimens were fixed in 10% buffered formaldehyde and then embedded in paraffin. The sections (4 μm thick) were cut from the tissue blocks and stained with hematoxylin and eosin (H&E). The presence of FCA, which are phenotypically altered hepatocytes showing swollen and basophilic cytoplasm and hyperchromatic nuclei, was determined according to the criteria described previously (26). The multiplicity of the FCA was assessed on a per unit area basis (per cm^2). Fatty metamorphosis (% of fatty degeneration) was determined on the H&E-stained liver section using the BZ-Analyzer-II software (KEYENCE, Osaka, Japan (27)).

To evaluate adipocyte size, 10 adipocytes from each stained section (a total of 50 adipocytes) in each group were analyzed using a fluorescence microscope BZ-9000 (KEYENCE). Adipocyte size was measured and averaged using the BZ-Analyzer-II (KEYENCE). The unit of mean adipocyte size was square micrometers (μm^2).

Immunohistochemical analysis of proliferating cell nuclear antigen and F4/80

Immunohistochemical staining of proliferating cell nuclear antigen (PCNA), a G_1-to-S phase marker, was performed to estimate the cell proliferative activity of FCA using an anti-PCNA antibody (1:100; Santa Cruz Biotechnology, Santa Cruz, CA, USA). On the PCNA-immunostained sections, the cells with intensively reacted nuclei were considered to be positive for PCNA, and the indices (%) were calculated in 20 FCA randomly selected from each group (28).

Immunohistochemical staining to detect F4/80, a mature macrophage marker, was also performed to estimate the presence of macrophage infiltration in the WAT. After endogenous peroxidase activity was blocked with H_2O_2, the sections were incubated with a F4/80 primary antibody (1:50; AbD Serotec, Oxford, UK) for 30 min at 37°C. Subsequently, the sections were incubated with biotinylated secondary antibodies against the primary antibodies (Dako, Carpinteria, CA, USA) and then incubated with avidin-coupled peroxidase. The sections were then developed with 3,3′-diaminobenzidine using Dako Liquid DAB Substrate-Chromogen System (Dako) and counterstained with hematoxylin.

Hepatic lipid analysis

Approximately 200 mg of frozen liver was homogenized, and the lipids were extracted using a chloroform:methanol (2:1 v/v) solution, as described by Folch *et al.* (29). The levels of triglycerides in the livers of the mice were measured using the triglyceride E-test kit (Wako Pure Chemical, Osaka, Japan) according to the manufacturer's protocol (17).

RNA extraction and quantitative real-time reverse transcription–PCR analysis

Total RNA was isolated from the livers and adipose tissues of the mice using the RNeasy Mini Kit and RNeasy Lipid Tissue Mini Kit (Qiagen, Hilden, Germany), respectively. Total RNA (1 μg) was used for the synthesis of the first strand of complementary DNA using the SuperScript III First-Strand Synthesis System (Invitrogen, Carlsbad, CA, USA). Quantitative real-time reverse transcription (RT)-PCR was performed using specific primer sets that amplify PCNA, c-*fos*, interleukin (IL)-6, IL-1β, IL-18, tumor necrosis factor-α (TNF-α), monocyte chemoattractant protein-1 (MCP-1), adiponectin, PPAR-α, PPAR-γ, Bax, Bcl-2, $p21^{CIP1}$, $p27^{KIP1}$, cyclin D1 and β-actin genes. The sequences of these primers, which are obtained from the PrimerBank (http://pga.mgh.harvard.edu/primerbank/), are given in Table I. Each sample was analyzed on a LightCycler 1.0 (Roche Diagnostics, GmbH, Mannheim, Germany) with SYBR Premix Ex Taq (TaKaRa Bio, Shiga, Japan). The expression level of each gene was normalized to the β-actin expression level using the standard curve method (17).

Statistical analysis

All data were expressed as the mean ± the standard error mean (SEM). Differences between the two groups were analyzed using Student's *t*-test. All analyses were conducted using JMP 8.0 (SAS Institute Inc., Cary, NC, USA). Values with $P < 0.05$ were considered to be significant.

Table I. Primer sequences

Gene		Primer sequence
PCNA	F	5′-TTTGAGGCACGCCTGATCC-3′
	R	5′-GGAGACGTGAGACGAGTCCAT-3′
c-fos	F	5'-CGGGTTTCAACGCCGACTA-3'
	R	5′-TTGGCACTAGAGACGGACAGA-3′
IL-6	F	5′-CTGCAAGAGACTTCCATCCAG-3′
	R	5-AGTGGTATAGACAGGTCTGTTGG-3′
IL-1β	F	5′-GCAACTGTTCCTGAACTCAACT-3′
	R	5-ATCTTTTGGGGTCCGTCAACT-3′
IL-18	F	5′-GTGAACCCCAGACCAGACTG-3′
	R	5′-CCTGGAACACGTTTCTGAAAGA-3′
TNF-α	F	5′-CAGGCGGTGCCTATGTCTC-3′
	R	5′-CGATCACCCCGAAGTTCAGTAG-3′
adiponectin	F	5′-TGTTCCTCTTAATCCTGCCCA-3′
	R	5′-CCAACCTGCACAAGTTCCCTT-3′
PPAR-α	F	5′-AGAGCCCCATCTGTCCTCTC-3′
	R	5′-ACTGGTAGTCTGCAAAACCAAA-3′
PPAR-γ	F	5′-TCGCTGATGCACTGCCTATG-3′
	R	5′-GAGAGGTCCACAGAGCTGATT-3′
MCP-1	F	5′-TTAAAAACCTGGATCGGAACCAA-3′
	R	5′-GCATTAGCTTCAGATTTACGGGT-3′
Bax	F	5′-AGACAGGGGCCTTTTTGCTAC-3′
	R	5′-AATTCGCCGGAGACACTCG-3′
Bcl-2	F	5′-ATGCCTTTGTGGAACTATATGGC-3′
	R	5′-GGTATGCACCCAGAGTGATGC-3′
$p21^{CIP1}$	F	5′-CCTGGTGATGTCCGACCTG-3′
	R	5′-CCATGAGCGCATCGCAATC-3′
$p27^{KIP1}$	F	5′-TCAAACGTGAGAGTGTCTAACG-3′
	R	5′-CCGGGCCGAAGAGATTTCTG-3′
Cyclin D1	F	5′-GCGTACCCTGACACCAATCTC-3′
	R	5′-ACTTGAAGTAAGATACGGAGGGC-3′
β-actin	F	5′-GGCTGTATTCCCCTCCATCG-3′
	R	5′-CCAGTTGGTAACAATGCCATGT-3′

Results

General observations

Body, liver, kidney and fat (WAT of the periorchis and retroperitoneum) weights and hepatic triglyceride levels of the two groups measured at the end of the study are listed in Table II. The mean liver weight and mean level of triglycerides in the livers of the mice in the BCAA supplementation group were found to be significantly less than those in the mice in the casein-treated group ($P < 0.05$). BCAA supplementation also improved macrovesicular steatosis, which was observed in the casein-fed mice ($P < 0.05$, Figure 1A), suggesting that BCAA supplementation inhibits hepatomegaly by improving the accumulation of lipids in the liver. Other measurements did not differ significantly between the two groups. All of the mice remained healthy, and no clinical signs indicating toxicity of BCAA were observed during the experiment. Histopathologically, there were no

Table II. Body, liver, kidney and fat weights and hepatic triglyceride levels of the experimental mice

Treatment	No. of mice	Body wt (g)	Relative wt (g/100 g body wt) of			Hepatic triglyceride (mg/100 mg liver tissue)
			Liver	Kidney	Fat[a]	
Casein	5	67.9±7.9[b]	7.1±1.5	0.9±0.1	9.1±2.1	13.9±2.8
BCAA	5	68.4±2.7	5.1±0.6[c]	0.9±0.1	11.0±2.5	6.8±4.4c

[a]White adipose tissue of the periorchis and retroperitoneum.
[b]Mean ± SEM.
[c]$P < 0.05$.

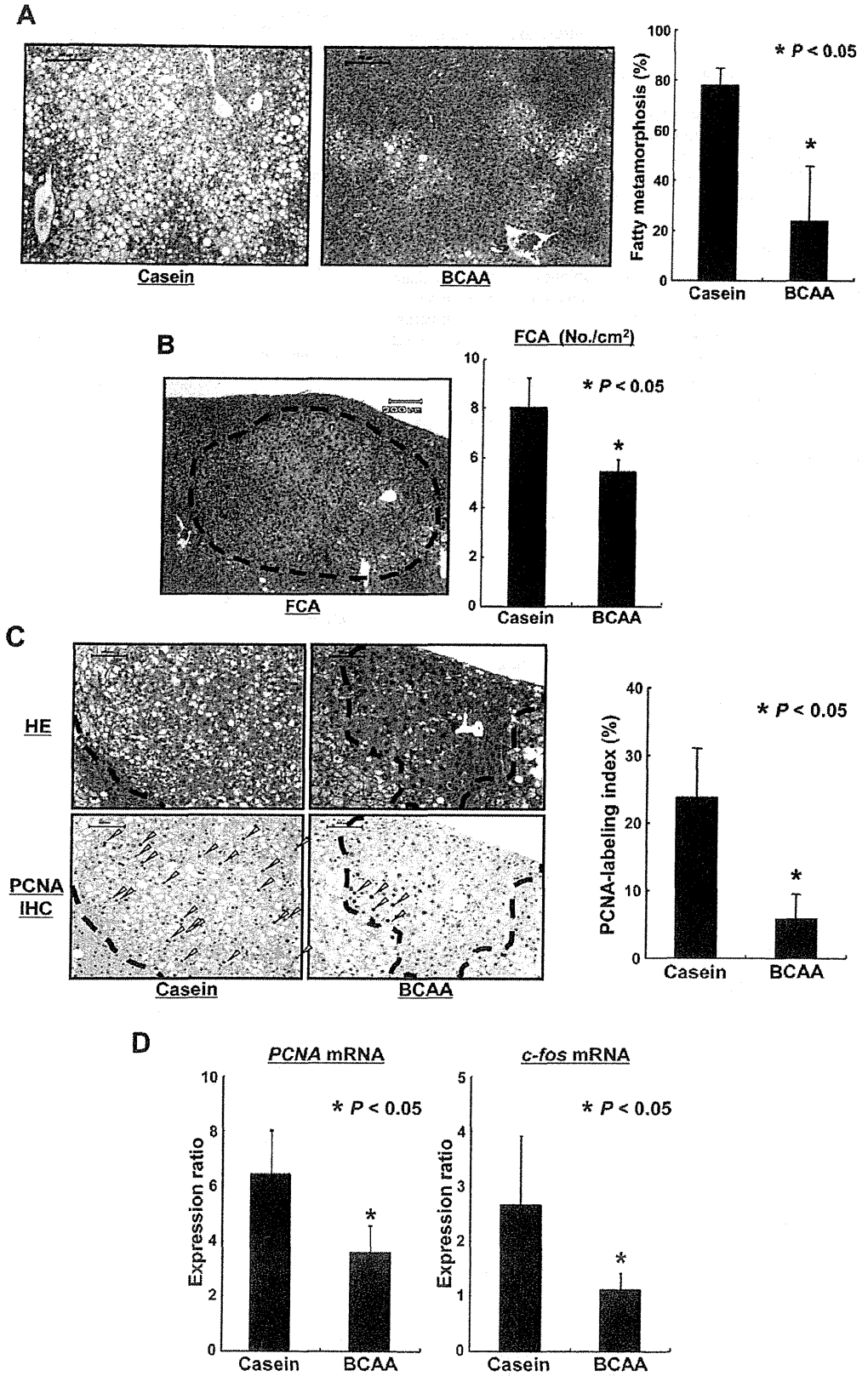

Fig. 1. Effects of BCAA supplementation on the hepatic steatosis, development of FCA, and on the expression of PCNA and c-*fos* mRNA in the livers of the *db/db* mice. (A) Histopatology (H&E staining) and a morphometric analysis of fatty metamorphosis in the liver of the casein-supplemented and the BCAA-supplemented *db/db* mice. (B) A representative photograph of FCA that spontaneously developed in the *db/db* mice (H&E staining) and the average number of FCA in the casein-supplemented and the BCAA-supplemented groups. (C) Representative photographs of H&E staining and the PCNA-immunohistochemical analysis of the FCA developed in the livers of the casein-supplemented and the BCAA-supplemented mice (left panels). The PCNA-labeling indices of the FCA developed in the livers of each group were determined by counting the PCNA-positive nuclei (arrowheads) in the FCA (right panel). * $P < 0.05$ versus the casein-supplemented group. (D) The expression levels of PCNA and c-*fos* mRNA in the liver of the casein-supplemented and the BCAA-supplemented mice were examined by quantitative real-time RT–PCR using specific primers. The values are expressed as the mean ± the SEM. *$P < 0.05$ versus the casein-supplemented group.

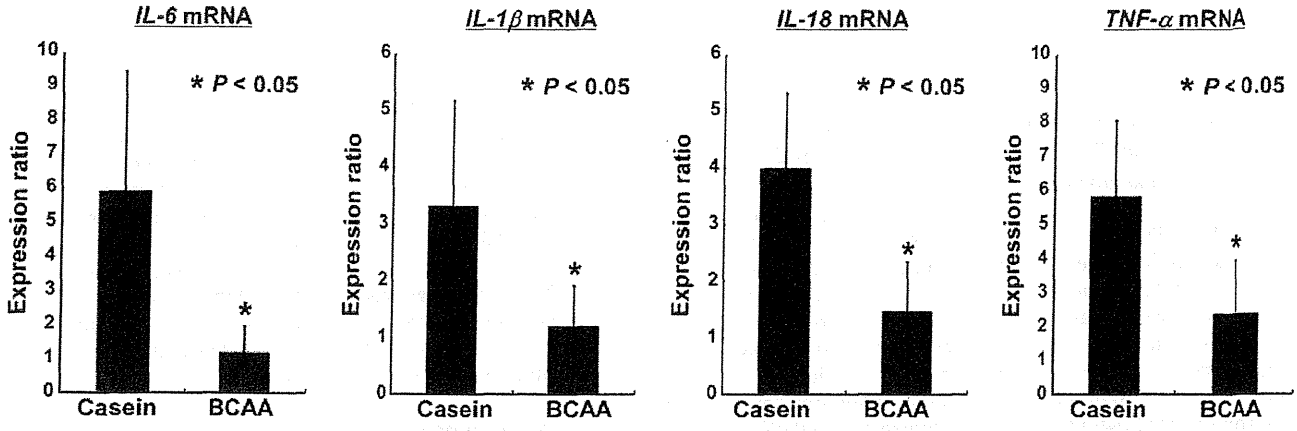

Fig. 2. Effect of BCAA supplementation on the expression of IL-6, IL-1β, IL-18 and TNF-α mRNA in the livers of the *db/db* mice. The expression levels of IL-6, IL-1β, IL-18 and TNF-α mRNA in the liver of the casein-supplemented and the BCAA-supplemented mice were examined by quantitative real-time RT–PCR using specific primers. The values are expressed as the mean ± the SEM. *$P < 0.05$ versus the casein-supplemented group.

findings suggesting any toxicity of BCAA to major organs, including the liver, kidney and spleen.

Effects of BCAA supplementation on the spontaneous development of FCA, the proliferation activity in FCA and the expression levels of PCNA and c-fos messenger RNA in the livers of the db/db mice

At sacrifice, FCA developed in the liver of all experimental mice regardless of the treatment. It was found that supplementation with BCAA significantly decreased the number of FCA when compared with casein supplementation ($P < 0.05$, Figure 1B). An immunohistochemical analysis to detect PCNA showed the mean PCNA-labeling index for FCA in the BCAA-supplemented mice to be significantly lower than that in the casein-supplemented mice ($P < 0.05$, Figure 1C). In the whole liver, BCAA supplementation also inhibited the expression levels of PCNA and c-*fos* messenger RNA (mRNA) in comparison with casein supplementation

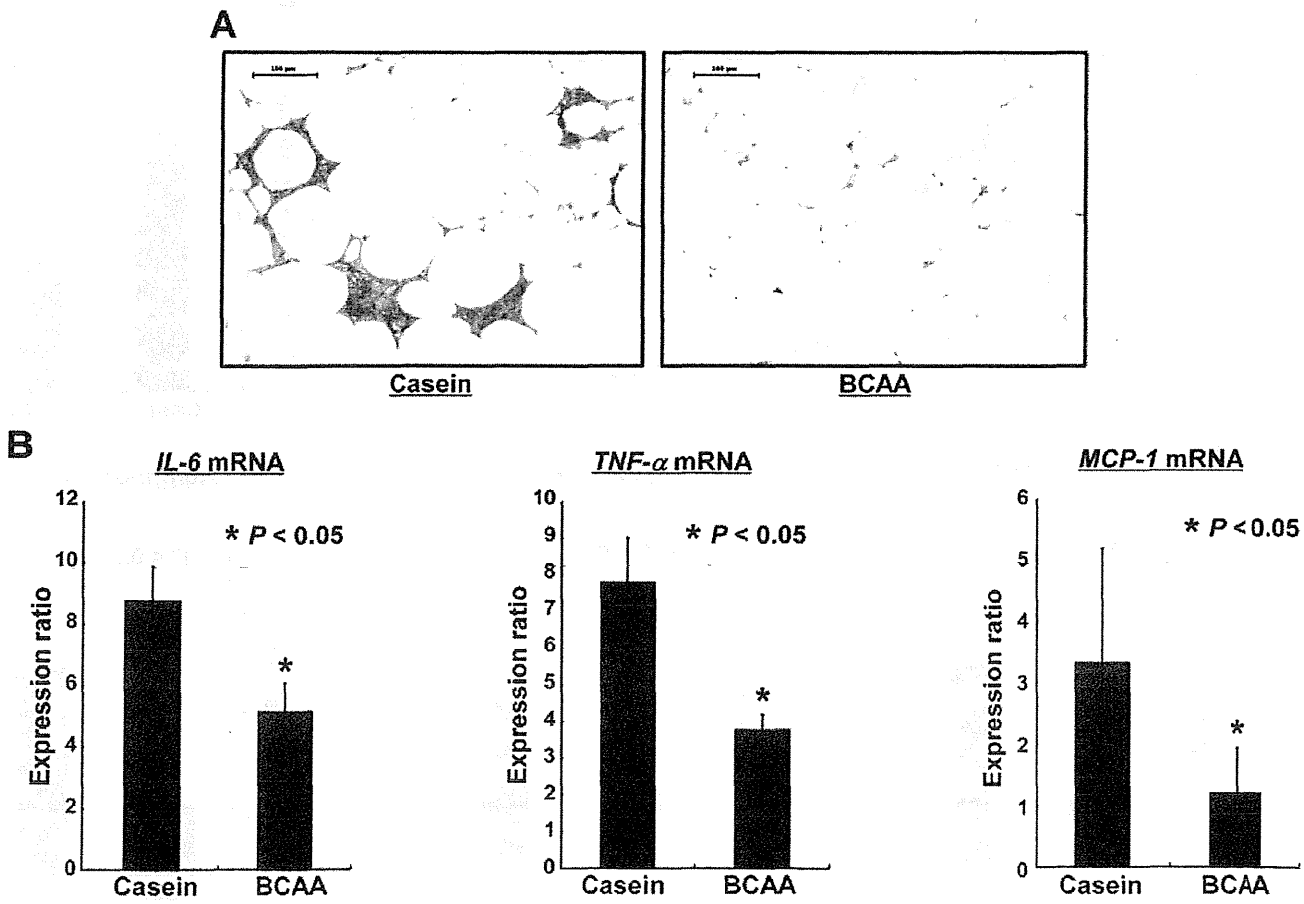

Fig. 3. Effect of BCAA supplementation on macrophage infiltration and the expression of IL-6, TNF-α and MCP-1 mRNA in the WAT of the *db/db* mice. (A) The F4/80 immunohistochemical analyses were performed in the periorchis WAT of the casein-supplemented and the BCAA-supplemented mice to show macrophage infiltration. (B) The expression levels of IL-6, TNF-α and MCP-1 mRNA in the periorchis WAT of the casein-supplemented and the BCAA-supplemented mice were examined by quantitative real-time RT–PCR using specific primers. The values are expressed as the mean ± the SEM. *$P < 0.05$ versus the casein-supplemented group.

($P < 0.05$, Figure 1D). These findings suggest that BCAA supplementation prevents the development of FCA, at least in part, by reducing cell proliferation.

Effects of BCAA supplementation on the expression levels of IL-6, IL-1β, IL-18 and TNF-α mRNA in the livers of the db/db mice

Chronic inflammation induced by the excessive production of storage lipids plays a role in obesity-related liver carcinogenesis (2,6–10). Therefore, the effects of BCAA supplementation on the expression levels of proinflammatory cytokines IL-6, IL-1β, IL-18 and TNF-α mRNA, which are central mediators of chronic inflammatory diseases (2,6–10), in the livers of the *db/db* mice were determined. Quantitative real-time RT–PCR revealed that in comparison with the casein-supplemented mice, the experimental mice showed significantly decreased expression levels of mRNA in the liver following BCAA supplementation ($P < 0.05$, Figure 2). These findings suggest that BCAA supplementation attenuates chronic inflammation in the livers of obese and diabetic *db/db* mice.

Effects of BCAA supplementation on macrophage infiltration and the expression level of IL-6, TNF-α and MCP-1 mRNA in the WAT of the db/db mice

Macrophages play important roles in inflammation in obese adipose tissue (21,22). Therefore, whether BCAA supplementation attenuates chronic inflammation or inhibits increased infiltration of macrophages in WAT was examined. Immunohistochemica analysis performed with an antibody to F4/80 revealed the presenc of apparent macrophage infiltration in the periorchis WAT of th casein-supplemented *db/db* mice; however, the infiltration wa markedly inhibited by BCAA supplementation (Figure 3A) The expression levels of IL-6 and TNF-α mRNA in the WA were also reduced by BCAA supplementation. Additionally supplementation with BCAA significantly inhibited the expressio of MCP-1 mRNA ($P < 0.05$, Figure 3B), which plays a role in th recruitment of macrophages into obese adipose tissue (30,31) These findings suggest that inhibition of macrophage infiltratio and subsequent attenuation of chronic inflammation in WAT b BCAA supplementation are, at least in part, associated with th suppression of MCP-1 expression.

Effects of BCAA supplementation on adipocyte size and expression levels of PPAR-α, PPAR-γ, and adiponectin mRNA in the WAT of the db/db mice

The induction of inflammation in obese adipose tissue is associated with increased adipocyte size (21,22). Therefore, whether BCAA supplementation alters the histology of WAT was next examined. Histological analysis showed that in addition to the inhibition of macrophage infiltration, BCAA supplementation reduced the size of adipocyte (Figure 4A). The average adipocyte size observed in the BCAA-supplemented mice was significantly smaller than that observed in the casein-supplemented mice ($P < 0.05$, Figure 4B).

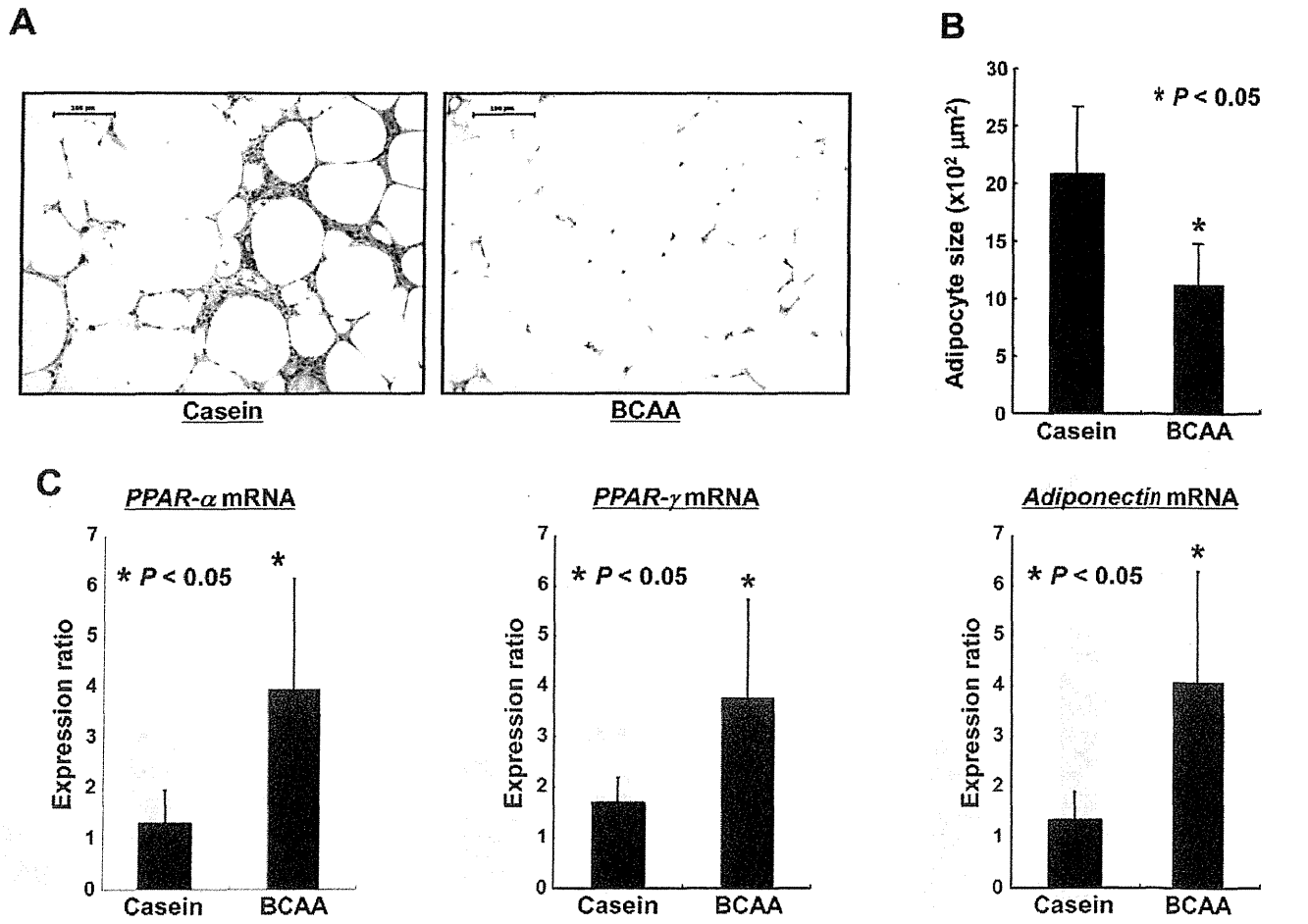

Fig. 4. Effect of BCAA supplementation on adipocyte size and the expression of PPAR-α, PPAR-γ and adiponectin mRNA in the WAT of the *db/db* mice. (A) The histopathology of the periorchis WAT of the casein-supplemented and the BCAA-supplemented mice (H&E staining). (B) The H&E staining images of the adipose tissues were analyzed using a fluorescence microscope BZ-9000, and adipocyte size was measured using a BZ-Analyzer-II. (C) The expression levels of PPAR-α, PPAR-γ and adiponectin mRNA in the periorchis WAT of the casein-supplemented and the BCAA-supplemented mice were examined by quantitative real-time RT–PCR using specific primers. The values are expressed as the mean ± the SEM. *$P < 0.05$ versus the casein-supplemented group.

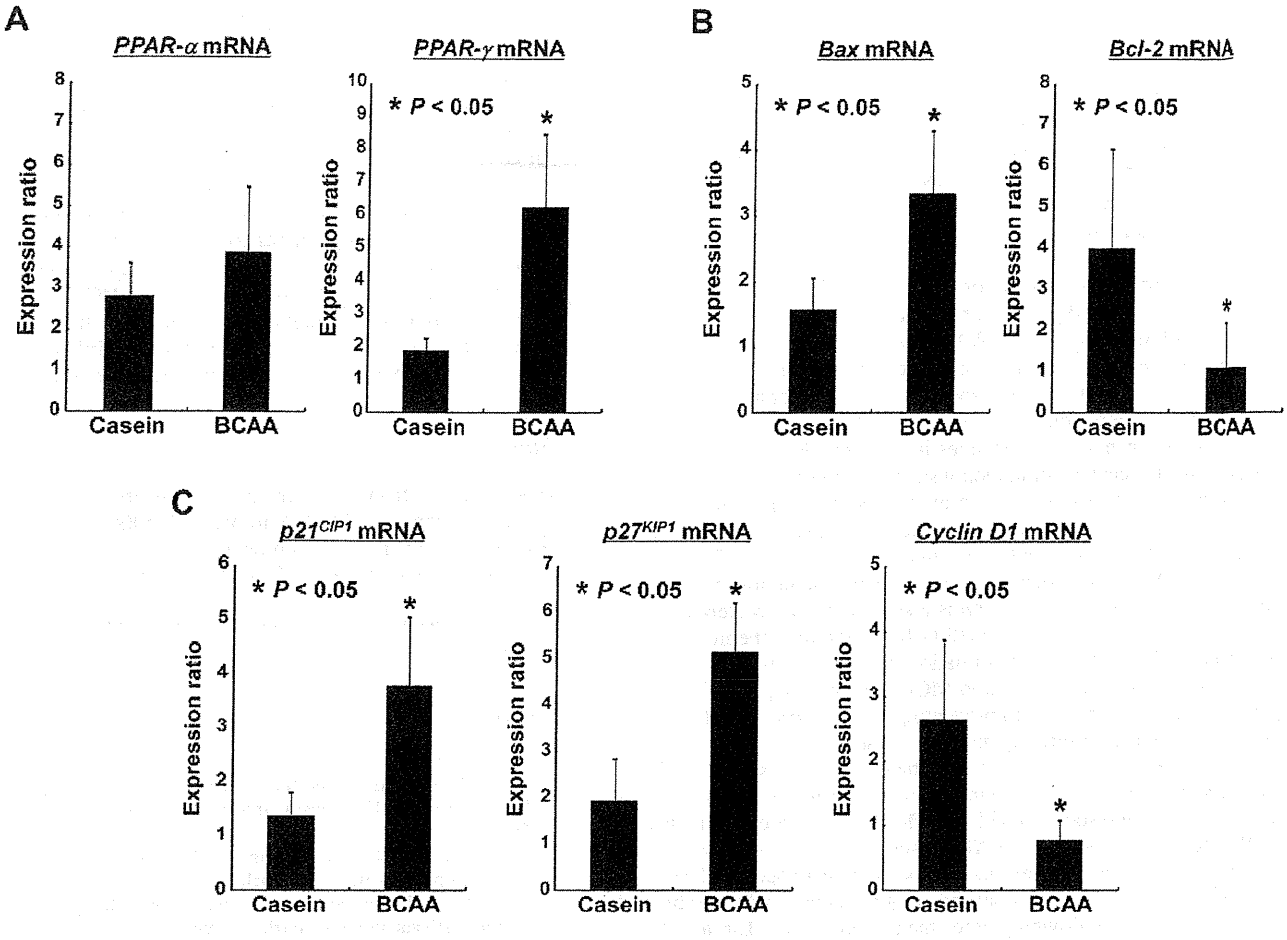

Fig. 5. Effect of BCAA supplementation on the expression of PPAR-α, PPAR-γ, Bax, Bcl-2, $p21^{CIP1}$, $p27^{KIP1}$ and cyclin D1 mRNA in the livers of the *db/db* mice. The expression levels of (A) PPAR-α and PPAR-γ, (B) Bax and Bcl-2 and (C) $p21^{CIP1}$, $p27^{KIP1}$ and cyclin D1 mRNA in the liver of the casein-supplemented and the BCAA-supplemented mice were examined using quantitative real-time RT–PCR with specific primers. The values are expressed as the mean ± SEM. *$P < 0.05$ versus the casein-supplemented group.

Moreover, BCAA supplementation increased the expression of PPAR-α mRNA, which can be a key regulator of inflammatory signaling (23,24), in the WAT of the *db/db* mice. Furthermore, the expression levels of PPAR-γ, a master regulator of adipocyte differentiation, and its downstream adiponectin mRNA, which also possesses the ability to suppress proinflammatory signaling (24,25), in the WAT were both significantly upregulated by BCAA supplementation ($P < 0.05$, Figure 4C).

Effects of BCAA supplementation on the expression levels of PPAR-α, PPAR-γ, Bax, Bcl-2, $p21^{CIP1}$, $p27^{KIP1}$ and cyclin D1 mRNA in the livers of the db/db mice

Recent studies have revealed the activation of PPAR-γ to exert a beneficial effect against HCC by inducing apoptosis and cell-cycle arrest (32,33). Therefore, in addition to the WAT (Figure 4C), whether BCAA supplementation also increases the expression levels of PPAR-γ in the liver was next examined. The expression levels of PPAR-γ mRNA in the liver were found to be significantly increased by BCAA supplementation ($P < 0.05$), whereas this agent did not alter the levels of PPAR-α mRNA (Figure 5A). Supplementation with BCAA increased the levels of Bax mRNA, which accelerates apoptosis, and decreased the levels of Bcl-2 mRNA, an anti-apoptotic member of the Bcl-2 family, in the livers of the experimental mice (Figure 5B, $P < 0.05$). There were also significant increases in the expression levels of $p21^{CIP1}$ and $p27^{KIP1}$ mRNA and decreases in the levels of cyclin D1 mRNA in the livers of the mice supplemented with BCAA (Figure 5C, $P < 0.05$).

Discussion

Obesity, which is implicated in the development of NAFLD and NASH, has been shown to increase the risk of developing HCC (1–5). The present study, a NAFLD mice model in which obesity and severe steatosis were developed, clearly indicates that dietary supplementation with BCAA effectively prevents the spontaneous development of liver preneoplastic lesions in *db/db* mice through the inhibition of cell proliferation. These findings are consistent with our recent report that BCAA supplementation suppresses the chemically induced liver tumorigenesis in obese mice by improving insulin resistance (17). We considered that the results of the present study showed an equivalent significance to those of the previous experiment (17) because NAFLD that has not yet progressed to NASH can induce hepatocyte proliferation and hepatic hyperplasia, both of which initiate the hepatic neoplastic process in obesity (34). Therefore, targeting NAFLD, a hyperproliferative field, through intervention using specific agents such as BCAA supplementation might be an effective strategy for preventing obesity-related liver carcinogenesis.

In various obesity-related metabolic disorders, substantial evidence has shown that chronic inflammation caused by obesity contributes to the progression of NAFLD to NASH and finally to HCC (2,6–10). Hepatic steatosis, which is a source of inflammation, also promotes the development of HCC (8,9). Therefore, reduction of lipid accumulation and attenuation of chronic inflammation in the liver achieved by BCAA supplementation play a critical role in the suppression of the spontaneous development of hepatic neoplastic lesions in obese mice. The inhibition of the expression of IL-6 and TNF-α by BCAA supplementation is particularly important in the suppression of the

spontaneous development of hepatic neoplastic lesions because increases in these proinflammatory cytokines, which are accompanied by lipid accumulation in the liver, are critically involved in obesity-related liver carcinogenesis (2,6–10). The preventive effects of obesity-related liver tumorigenesis by targeting IL-6 and TNF-α expression and liver steatosis are also demonstrated in other rodent studies (28,35,36). In addition, the alleviation of hepatic steatosis with BCAA supplementation, which might be associated with the effects of improving insulin resistance (13), is consistent with previous reports (17,20).

In addition to the benefits observed in the liver, the present study also showed that BCAA supplementation significantly attenuates chronic inflammation in the WAT of *db/db* mice. Macrophage infiltration into WAT, which is accompanied by IL-6 and TNF-α production, is an early contributing event for the development of chronic low-grade systemic inflammation (21,22). MCP-1 plays a crucial role in the recruitment of macrophages into obese adipose tissue (30,31). MCP-1 is also capable of inducing steatosis in hepatocytes, indicating that secretion of this chemokine by adipose tissue may induce steatosis not only by recruiting macrophages but also by acting directly on hepatocytes (37). In addition, upregulation of IL-6, TNF-α and MCP-1 in WAT is critically involved in the induction of systemic insulin resistance (21,22), which is a key factor for accelerating obesity-related liver carcinogenesis (2,6–10). Therefore, the inhibition of enhanced adipose tissue inflammation, that is increased macrophage infiltration and IL-6, TNF-α and MCP-1 expression, by BCAA supplementation is important in preventing the development of steatosis and subsequent liver tumorigenesis in obese mice.

The present study demonstrated that adipocyte size in BCAA-supplemented mice is much smaller than that in control mice. This finding might be associated with the effects of BCAA on the induction of PPAR-α and PPAR-γ in WAT because activation of these nuclear receptors significantly prevents adipocyte hypertrophy (24,38). An increase in the number of small adipocytes induces adiponectin and its receptors, which downregulates the production of IL-6 and TNF-α, thereby reducing obesity-related inflammation in adipose tissue (24,25). A lack of adiponectin enhances the progression of hepatic steatosis and tumor formation in a mice model of NASH (39), whereas this adipokine alleviates hepatic steatosis by decreasing TNF-α production (40). Moreover, the induction of adiponectin plays a role in the suppression of chemically induced liver tumorigenesis in obese mice (28). Therefore, in the present study, the effects of BCAA on the upregulation of PPAR-α, PPAR-γ and adiponectin achieved by inhibiting adipocyte hypertrophy may contribute to preventing obesity-related liver tumorigenesis.

In addition to the WAT, the present study also showed the first evidence that BCAA supplementation increases the mRNA level of PPAR-γ, but not that of PPAR-α, in the livers of obese mice. The precise mechanisms underlying the upregulation of the expression of PPAR-γ in the liver by BCAA have not yet been clarified. However, these findings are significant when considering the prevention of liver carcinogenesis because PPAR-γ is regarded to be an antitumorigenic factor in HCC, whereas the role of PPAR-α in HCC development is contradictory (32,33,41). The overexpression of PPAR-γ suppresses the growth of HCC cells by reducing cell proliferation and inducing apoptosis (32). The activation of PPAR-γ by its ligand also inhibits the proliferation of HCC cells by upregulating the $p21^{CIP1}$ and $p27^{KIP1}$ expression, which thus leads to the G_1 arrest of the cell cycle (33). These reports (32,33), together with the results of the present study showing that BCAA supplementation increases the expression of PPAR-γ, Bax, $p21^{CIP1}$ and $p27^{KIP1}$ mRNA and decreases the expression of Bcl-2 and cyclin D1 mRNA, suggest that the induction of apoptosis and regulation of cell-cycle progression induced by BCAA via the upregulation of PPAR-γ in the liver may also help to inhibit the development of FCA.

Finally, it should be noted again that improved insulin resistance achieved from BCAA supplementation, which has been demonstrated in several basic and clinical studies (13,16), is critical to suppress the development of neoplasms in both the liver and the colon of obese mice (17,18). Because chronic inflammation occurring in WAT plays a role in systemic insulin resistance (30,31), BCAA supplementation might prevent the spontaneous development of hepatic preneoplastic lesions via the attenuation of adipocyte inflammation and the subsequent improvement of insulin resistance. These findings suggest that in addition to the liver, as shown in the present and previous studies (17,42), WAT might be a critical target for BCAA to exert chemopreventive properties in obesity-related liver carcinogenesis.

In conclusion, supplementation with BCAA may be an effective strategy for the chemoprevention of HCC, especially in obese patients who are at an increased risk of developing HCC. The results of the present study further strengthen our hypothesis that targeting obesity-induced pathologic conditions, such as chronic inflammation, might be effective for preventing liver carcinogenesis in obese individuals (11).

Funding

Grants-in-Aid from the Ministry of Education, Science, Sports and Culture of Japan (22790638 to M.S., 21590838 to H.M.); Grant-in-Aid for the 3rd Term Comprehensive 10-Year Strategy for Cancer Control from the Ministry of Health, Labor and Welfare of Japan.

Conflict of Interest Statement: The authors declare that they have no competing interests.

References

1. El-Serag,H.B. *et al.* (2007) Hepatocellular carcinoma: epidemiology and molecular carcinogenesis. *Gastroenterology*, **132**, 2557–2576.
2. Sun,B. *et al.* (2012) Obesity, inflammation, and liver cancer. *J. Hepatol.*, **56**, 704–713.
3. Muto,Y. *et al.* (2006) Overweight and obesity increase the risk for liver cancer in patients with liver cirrhosis and long-term oral supplementation with branched-chain amino acid granules inhibits liver carcinogenesis in heavier patients with liver cirrhosis. *Hepatol. Res.*, **35**, 204–214.
4. Imai,K. *et al.* (2010) Insulin resistance raises the risk for recurrence of stage I hepatocellular carcinoma after curative radiofrequency ablation in hepatitis C virus-positive patients: A prospective, case series study. *Hepatol. Res.*, **40**, 376–382.
5. El-Serag,H.B. *et al.* (2001) The role of diabetes in hepatocellular carcinoma: a case-control study among United States Veterans. *Am. J. Gastroenterol.*, **96**, 2462–2467.
6. Siegel,A.B. *et al.* (2009) Metabolic syndrome and hepatocellular carcinoma: two growing epidemics with a potential link. *Cancer*, **115**, 5651–5661.
7. Ratziu,V. *et al.* (2002) Survival, liver failure, and hepatocellular carcinoma in obesity-related cryptogenic cirrhosis. *Hepatology*, **35**, 1485–1493.
8. Smedile,A. *et al.* (2005) Steatosis and hepatocellular carcinoma risk. *Eur. Rev. Med. Pharmacol. Sci.*, **9**, 291–293.
9. Powell,E.E. *et al.* (2005) Steatosis: co-factor in other liver diseases. *Hepatology*, **42**, 5–13.
10. Park,E.J. *et al.* (2010) Dietary and genetic obesity promote liver inflammation and tumorigenesis by enhancing IL-6 and TNF expression. *Cell*, **140**, 197–208.
11. Shimizu,M. *et al.* (2012) Nutraceutical approach for preventing obesity-related colorectal and liver carcinogenesis. *Int. J. Mol. Sci.*, **13**, 579–595.
12. Moriwaki,H. *et al.* (2004) Branched-chain amino acids as a protein- and energy-source in liver cirrhosis. *Biochem. Biophys. Res. Commun.*, **313**, 405–409.
13. Kawaguchi,T. *et al.* (2011) Branched-chain amino acids as pharmacological nutrients in chronic liver disease. *Hepatology*, **54**, 1063–1070.
14. Muto,Y. *et al.* (2005) Effects of oral branched-chain amino acid granules on event-free survival in patients with liver cirrhosis. *Clin. Gastroenterol. Hepatol.*, **3**, 705–713.
15. Marchesini,G. *et al.* (2003) Nutritional supplementation with branched-chain amino acids in advanced cirrhosis: a double-blind, randomized trial. *Gastroenterology*, **124**, 1792–1801.
16. Kawaguchi,T. *et al.* (2008) Branched-chain amino acid-enriched supplementation improves insulin resistance in patients with chronic liver disease. *Int. J. Mol. Med.*, **22**, 105–112.
17. Iwasa,J. *et al.* (2010) Dietary supplementation with branched-chain amino acids suppresses diethylnitrosamine-induced liver tumorigenesis in obese and diabetic C57BL/KsJ-db/db mice. *Cancer Sci.*, **101**, 460–467.

18. Shimizu,M. *et al.* (2009) Supplementation with branched-chain amino acids inhibits azoxymethane-induced colonic preneoplastic lesions in male C57BL/KsJ-db/db mice. *Clin. Cancer Res.*, **15**, 3068–3075.
19. Hagiwara,A. *et al.* (2012) Branched-chain amino acids prevent insulin-induced hepatic tumor cell proliferation by inducing apoptosis through mTORC1 and mTORC2-dependent mechanisms. *J. Cell. Physiol.*, **227**, 2097–2105.
20. Arakawa,M. *et al.* (2011) The effects of branched-chain amino acid granules on the accumulation of tissue triglycerides and uncoupling proteins in diet-induced obese mice. *Endocr. J.*, **58**, 161–170.
21. Weisberg,S.P. *et al.* (2003) Obesity is associated with macrophage accumulation in adipose tissue. *J. Clin. Invest.*, **112**, 1796–1808.
22. Xu,H. *et al.* (2003) Chronic inflammation in fat plays a crucial role in the development of obesity-related insulin resistance. *J. Clin. Invest.*, **112**, 1821–1830.
23. Li,P. *et al.* (2005) Metabolic and cellular plasticity in white adipose tissue II: role of peroxisome proliferator-activated receptor-alpha. *Am. J. Physiol. Endocrinol. Metab.*, **289**, E617–E626.
24. Tsuchida,A. *et al.* (2005) Peroxisome proliferator-activated receptor (PPAR)alpha activation increases adiponectin receptors and reduces obesity-related inflammation in adipose tissue: comparison of activation of PPARalpha, PPARgamma, and their combination. *Diabetes*, **54**, 3358–3370.
25. Ouchi,N. *et al.* (2007) Adiponectin as an anti-inflammatory factor. *Clin. Chim. Acta*, **380**, 24–30.
26. Frith,C.H. *et al.* (1994) Tumours of the liver. In *Pathology of Tumors in Laboratory Animals*. Vol. 2. IARC Scientific Publications, Lyon, pp. 223–270.
27. Suzuki,R. *et al.* (2007) Diet supplemented with citrus unshiu segment membrane suppresses chemically induced colonic preneoplastic lesions and fatty liver in male db/db mice. *Int. J. Cancer*, **120**, 252–258.
28. Shimizu,M. *et al.* (2011) Pitavastatin suppresses diethylnitrosamine-induced liver preneoplasms in male C57BL/KsJ-db/db obese mice. *BMC Cancer*, **11**, 281.
29. FOLCH,J. *et al.* (1957) A simple method for the isolation and purification of total lipides from animal tissues. *J. Biol. Chem.*, **226**, 497–509.
30. Kamei,N. *et al.* (2006) Overexpression of monocyte chemoattractant protein-1 in adipose tissues causes macrophage recruitment and insulin resistance. *J. Biol. Chem.*, **281**, 26602–26614.
31. Kanda,H. *et al.* (2006) MCP-1 contributes to macrophage infiltration into adipose tissue, insulin resistance, and hepatic steatosis in obesity. *J. Clin. Invest.*, **116**, 1494–1505.
32. Yu,J. *et al.* (2010) Inhibitory role of peroxisome proliferator-activated receptor gamma in hepatocarcinogenesis in mice and *in vitro*. *Hepatology*, **51**, 2008–2019.
33. Koga,H. *et al.* (2001) Involvement of p21(WAF1/Cip1), p27(Kip1), and p18(INK4c) in troglitazone-induced cell-cycle arrest in human hepatoma cell lines. *Hepatology*, **33**, 1087–1097.
34. Yang,S. *et al.* (2001) Hepatic hyperplasia in noncirrhotic fatty livers: is obesity-related hepatic steatosis a premalignant condition? *Cancer Res.*, **61**, 5016–5023.
35. Shimizu,M. *et al.* (2011) Acyclic retinoid inhibits diethylnitrosamine-induced liver tumorigenesis in obese and diabetic C57BLKS/J-+(db)/+Lepr(db) mice. *Cancer Prev. Res. (Phila).*, **4**, 128–136.
36. Shimizu,M. *et al.* (2011) Preventive effects of (-)-epigallocatechin gallate on diethylnitrosamine-induced liver tumorigenesis in obese and diabetic C57BL/KsJ-db/db Mice. *Cancer Prev. Res. (Phila).*, **4**, 396–403.
37. Clément,S. *et al.* (2008) Monocyte chemoattractant protein-1 secreted by adipose tissue induces direct lipid accumulation in hepatocytes. *Hepatology*, **48**, 799–807.
38. Yamauchi,T. *et al.* (2001) The mechanisms by which both heterozygous peroxisome proliferator-activated receptor gamma (PPARgamma) deficiency and PPARgamma agonist improve insulin resistance. *J. Biol. Chem.*, **276**, 41245–41254.
39. Kamada,Y. *et al.* (2007) Hypoadiponectinemia accelerates hepatic tumor formation in a nonalcoholic steatohepatitis mouse model. *J. Hepatol.*, **47**, 556–564.
40. Xu,A. *et al.* (2003) The fat-derived hormone adiponectin alleviates alcoholic and nonalcoholic fatty liver diseases in mice. *J. Clin. Invest.*, **112**, 91–100.
41. Reddy,J.K. *et al.* (1976) Hepatocellular carcinomas in acatalasemic mice treated with nafenopin, a hypolipidemic peroxisome proliferator. *Cancer Res.*, **36**, 1211–1217.
42. Yoshiji,H. *et al.* (2009) Branched-chain amino acids suppress insulin-resistance-based hepatocarcinogenesis in obese diabetic rats. *J. Gastroenterol.*, **44**, 483–491.

Received May 25, 2012; revised September 13, 2012; accepted September 20, 2012

The American Journal of Pathology, Vol. 182, No. 4, April 2013

ELSEVIER

The American Journal of
PATHOLOGY
ajp.amjpathol.org

GASTROINTESTINAL, HEPATOBILIARY, AND PANCREATIC PATHOLOGY

Tumor Suppressor APC Protein Is Essential in Mucosal Repair from Colonic Inflammation through Angiogenesis

Kazuto Yoshimi,* Takuji Tanaka,† Tadao Serikawa,* and Takashi Kuramoto*

From the Institute of Laboratory Animals, Graduate School of Medicine, Kyoto University, Kyoto; and Cancer Research and Prevention,† The Tohkai Cytopathology Institute, Gifu, Japan*

Accepted for publication December 24, 2012.

Address correspondence to Takashi Kuramoto, Ph.D., Institute of Laboratory Animals, Graduate School of Medicine, Kyoto University, Yoshidakonoe-cho, Sakyo-ku, Kyoto 606-8501, Japan. E-mail: tkuramot@anim.med.kyoto-u.ac.jp.

Mucosal repair after acute colonic inflammation is central to maintaining mucosal homeostasis. Failure of mucosal repair often leads to chronic inflammation, sometimes associated with inflammatory bowel disease (IBD). The adenomatous polyposis coli (*APC*) tumor suppressor gene regulates the Wnt signaling pathway, which is essential for epithelial development, and inactivation of *APC* facilitates colorectal cancer. Our previous study suggested that *APC* is involved in pathogenesis of colonic inflammation; however, its role in mucosal repair remains unknown. In this article, we report that colitis induced by dextran sodium sulfate persisted with delayed mucosal repair in Kyoto Apc Delta (KAD) rats lacking the APC C terminus. Defects in the repair process were accompanied by an absence of a fibrin layer covering damaged mucosa and reduced microvessel angiogenesis. APC was up-regulated in vascular endothelial cells (VECs) in inflamed mucosa in KAD and F344 (control) rats. The VECs of KAD rats revealed elevated cell adhesion and low-branched and short-length tube formation. We also found that DLG5, which is associated with IBD pathogenesis, was up-regulated in VECs in inflamed mucosa and interacted with the C terminus of APC. This finding suggests that loss of interaction between the APC C terminus and DLG5 affects VEC morphology and function and leads to persistence of colitis. Therefore, APC is essential for maintenance of intestinal mucosal homeostasis and can consequently contribute to IBD pathogenesis. *(Am J Pathol 2013, 182: 1263–1274; http://dx.doi.org/10.1016/j.ajpath.2012.12.005)*

Mucosal epithelial defense is an important system to prevent injuries induced by undigested substances, acid, ischemia, and microbial infection.[1,2] Once the mucosa is injured, the repair process—which is complex but primarily consists of the immune response, granulation tissue formation, angiogenesis, and epithelial regeneration—plays a central role to prevent further injuries.[3] Defects in such repair systems are a potential risk for persistent inflammation of the intestine or colon, which can lead to chronic inflammation, such as that seen in inflammatory bowel disease (IBD).

IBD, including ulcerative colitis and Crohn's disease, represents a chronic, relapsing and remitting inflammatory condition that affects individuals throughout life.[4] Patients with IBD are at risk of developing colorectal cancer.[5] Although it is widely accepted that genetic, environmental, and immunologic factors are involved,[6,7] the pathogenesis of IBD remains unclear. No completely effective therapeutic strategy has yet been established.

To investigate the pathogenesis of IBD, animal models of experimental colitis have been developed.[8] The dextran sodium sulfate (DSS) model is excellent for its resemblance to the clinical symptom of the IBD and for its ease of reproducibility and accessibility.[9] Providing drinking water containing DSS for several days induces colitis in rodents, which has characteristics similar to human ulcerative colitis, such as signs of diarrhea, gross rectal bleeding, weight loss, shortening of the colorectum, histologic features of multiple erosions, and inflammatory mucosal changes, occasionally including crypt abscess. Colitis is also predominant in the

Supported in part by a Grant-in-Aid for Cancer Research from the Ministry of Health, Labour and Welfare and Grants-in-Aid for Scientific Research from the Japan Society for the Promotion of Science (21300153 to T.K. and 0233639 to K.Y.).

The KAD (F344-*Apc*^{m1Kyo}) rat has been deposited in the National Bioresource Project-Rat in Japan (Institute of Laboratory Animals, Kyoto University).

http://dx.doi.org/10.1016/j.ajpath.2012.12.005

descending and sigmoid colons and the rectum and associated with alteration of intestinal flora. Some pathogenic and regulatory factors demonstrated in the DSS model, such as cytokines, growth factors, and inflammatory enzymes, have been exploited to develop future therapeutic strategies against IBD.[8]

Adenomatous polyposis coli (*APC*) has been identified as the causative gene of familial adenomatous polyposis of the colon, which is characterized by numerous polyps in the intestine.[10] Genetic studies using mutant mouse models indicate that *APC* is essential for development and that its inactivation facilitates tumorigenesis.[11]

APC is a 2843–amino acid polypeptide and is composed of multiple domains. Via these domains, APC can bind to various proteins, including the guanine-nucleotide-exchange factor ASEF1, the Wnt pathway component β-catenin, microtubules (MTs), the cytoskeletal regulator EB1, and homologs of the *Drosophila* disks large protein (DLG).[12] Most cancer-linked *APC* mutations occur at the central region of *APC* (the so-called mutation cluster region) and result in truncation of almost half of the C terminal region of the protein.[13] Because these truncations cause loss of the domains required for binding to β-catenin, MTs, EB1, and DLG, the interaction of APC with these molecules has been considered essential for its tumor-suppressing activity.

In 1999, Smits et al[14] developed a knockout mouse that carried a targeted mutation at codon 1638, *Apc*1638T (T for truncated). The resultant truncated APC protein contains β-catenin binding sites but lacks all of the C-terminus domains. $Apc^{1638T/1638T}$ mice survive to adulthood and are tumor free. Thus, the interaction of APC with β-catenin but not MTs, EB1, or DLG is critical in tumorigenesis. In addition, $Apc^{1638T/1638T}$ mice have growth retardation, reduced postnatal viability, the absence of preputial glands, and the formation of nipple-associated cysts.[14] Enlarged thyroid follicles and low responsiveness to thyroid-stimulating hormone are also found with $Apc^{1638T/1638T}$ mice.[15] Therefore, the C terminus of APC appears to be involved in the development of several tissues as described in this article; however, its physiologic function *in vivo* remains unclear.

We recently developed a mutant rat that carries a homozygous nonsense mutation at codon 2523 ($Apc^{\Delta 2523}$), which we call the Kyoto Apc Delta (KAD) rat.[16] The KAD rat expresses truncated APC protein that contains β-catenin binding sites but lacks the C terminus (321 amino acids in length), which can bind to MT, EB1, and DLG. KAD rats survive to adulthood and are free of intestinal tumors. However, when KAD rats received a single subcutaneous administration of 20 mg/kg of azoxymethane and 1 week later were given 2% DSS (in drinking water) for 1 week, they had a significantly higher incidence and multiplicity of colon tumors at week 15 compared with control F344 rats.[16,17] In contrast, KAD rats treated with azoxymethane only did not develop colon tumors (as assessed by the carcinogenesis test) by 15 weeks, similar to the azoxymethane-treated F344 rats. These findings suggest that the KAD rat is susceptible to inflammation provoked by the colitis-inducing agent and that the C terminus of APC appears to be involved in the pathogenesis of colitis.

In this study, we found that loss of the C terminus of APC affected the morphology and function of vascular endothelial cells (VECs) and led to a persistence of colitis. Our results reveal a new role of APC in the angiogenesis associated with mucosal repair of damage due to colitis.

Materials and Methods

Rats

F344/NSlc and KAD (homozygous for the $Apc^{\Delta 2523}$ mutation, official strain name: F344-Apc^{m1Kyo}) rats were obtained from Japan SLC, Inc. (Hamamatsu, Japan). KAD rats were backcrossed five times with female F344/NSlc rats to remove latent mutations induced by N-ethyl N-nitrosourea.[16] The rats were kept at the Institute of Laboratory Animals, Graduate School of Medicine, Kyoto University, under conditions of 50% humidity and a 14:10-hour light:dark cycle. They were fed a standard pellet diet (F-2, Oriental Yeast Co., Ltd, Tokyo, Japan) and tap water *ad libitum*.

Induction of Colitis

Male KAD rats (n = 30) and control F344/NSlc rats (F344 rats, n = 30) aged 5 weeks were given 2% DSS (molecular weight = 36,000-50,000 kDa) (MP Biochemicals, LLC., Solon, OH) in their drinking water for 1 week. The rats were divided into three groups: those sacrificed immediately after DSS treatment (week 1), those sacrificed 1 week after terminating the treatment (week 2), and those sacrificed 3 weeks after the treatment (week 4). The animals were sacrificed by cervical dislocation under anesthesia with isoflurane (Mylan Inc., New York, NY). The experimental procedures were approved by the Animal Research Committee of Kyoto University and were performed according to the Regulations on Animal Experimentation of Kyoto University.

Clinical assessment of inflammation involved monitoring the body weight and scoring the diarrhea and fecal blood for each rat.[18] The presence of diarrhea and fecal blood were scored on a scale of 1 and 2, respectively. The clinical inflammatory score for each animal was obtained by adding the diarrhea and fecal blood scores.

Histopathologic Analysis

An hour prior to sacrifice, the rats were injected intraperitoneally with 50 mg/kg of 5-bromo-2′-deoxyuridine (BrdU; Sigma, St. Louis, MO) to permit immunohistochemical (IHC) analysis of BrdU. On autopsy, the colorectum of each rat was resected and gently washed with PBS to remove feces. Half was used for a RT-PCR assay, and the other was fixed in 10% buffered formalin and embedded in paraffin for histopathologic analysis. Five serial sections of colonic

tissues (3 μm thick) were made: two sections stained with H&E to permit histologic examination and with phosphotungstic acid hematoxylin (PTAH) for detection of fibrin. Other sections were used for IHC with an LSAB2 Kit (Dako, Glostrup, Denmark). Anti-APC monoclonal antibody (EP701Y; Abcam, Cambridge, UK) and anti-CD31/platelet–endothelial cell adhesion molecule 1 polyclonal antibody (Santa Cruz Biotechnology, Santa Cruz, CA) were used as primary antibodies.

Cell proliferation in the inflamed mucosa was accessed by determination of the labeling index for BrdU-positive cells. The number of BrdU-positive cells was counted in at least 20 well-oriented crypts for each group. The labeling index was calculated by dividing the number of BrdU-positive cells by the total number of nucleated cells for each well-oriented crypt.

To investigate the localization of EB1, DLG1, and DLG5 in the inflamed colon, fluorescent immunochemistry was performed. Anti-CD31 polyclonal antibody (Santa Cruz Biotechnology) and anti-EB1, anti-DLG1, and anti-DLG5 polyclonal antibodies (Abcam) were used as primary antibodies. Alexa Fluor 488–conjugated anti-rabbit IgG antibody and Alexa Fluor 594–conjugated anti-mouse IgG antibody (1:200; Invitrogen, Carlsbad, CA) were used as secondary antibodies. Immunostained sections were visualized using a Biorevo immunofluorescence microscope (Keyence, Osaka, Japan).

Analysis of Colonic Microvasculature Density

Vascular density was calculated using an international consensus method to quantify angiogenesis, as previously described.[19] Briefly, CD31-stained distal colonic sections were scanned and the number of vessels within the mucosa was counted to identify the most vascularized area. Vascular density per field was obtained from at least five microphotographs of the most vascularized mucosa for each rat. Quantitative analysis of the data was performed using WinROOF software version 6.0 (Mitani Corp., Fukui, Fukui, Japan).

Real-Time PCR

Total RNA was isolated from inflamed mucosa of the distal colon 3 cm from the anus, and cDNA was synthesized. Real-time RT-PCR was performed using a Thermal Cycler Dice Real Time System with SYBR Premix Ex TaqII (Takara Bio Inc., Otsu, Shiga, Japan). The primers used were: *Tnfa*, 5′-AACTCGAGTGACAAGCCCGTAG-3′ and 5′-GTACCAC-CAGTTGGTTGTCTTTGA-3′; *Il1b*, 5′-GCTGTGGCAGC-TACCTATGTCTTG-3′ and 5′-AGGTCGTCATCATCCCA-CGAG-3′; *Il10*, 5′-CAGACCCACATGCTCCGAGA-3′ and 5′-CAAGGCTTGGCAACCCAAGTA-3′; *Ptgs2*, 5′-GCGA-CTGTTCCAAACCAGCA-3′ and 5′-TGGGTCGAACTTG-AGTTTGAAGTG-3′; *Ptges*, 5′-TACGCGGTGGCTGTCA-TCA-3′ and 5′-CTCCACATCTGGGTCACTCCTG-3′; *Ppia*, 5′-GGCAAATGCTGGACCAAACAC-3′ and 5′-AAACGC-TCCATGGCTTCCAC-3′. The number of target molecules was normalized against those of *Ppia* as an internal control.[20]

Reporter Gene Assay of Wnt Signaling

To measure Wnt signaling activity, rat embryonic fibroblasts (REFs) were isolated from E12.5 embryos of F344 and KAD rats in Dulbecco's modified Eagle's medium supplemented with 10% fetal bovine serum. REFs were then plated on 24-well culture plates 24 hours before transfection. Lipofectamine LTX (Invitrogen) was used to co-transfect REFs with pTOPFLASH or pFOPFLASH vector (Millipore, Billerica, MA) and pSV-β-Gal vector (Promega Corp., Madison, WI) as an internal control according to the manufacturer protocol. Cells in half of the plates were stimulated with 150 ng/mL of Wnt3a (R&D Systems Inc., Minneapolis, MN) 3 hours later. Luciferase activities were measured 24 hours after transfection with Luciferase Assay Systems (Promega).

Isolation of VECs

VECs were isolated from the thoracic aorta of four F344 and four KAD rats aged 8 weeks, as described previously.[21] VECs were cultured in MCDB 131 medium supplemented with epidermal growth factor, endothelial cell growth supplements, vascular endothelial growth factor, hydrocortisone, heparin, and 2% fetal bovine serum. Almost all cultured cells were of endothelial origin, as assessed by staining with Dil-Ac-LDL (Biomedical Technologies Inc., Stoughton, MA). All VECs were examined twice in all *in vitro* experiments to confirm their reproducibility.

Immunofluorescence Microscopy

Cells cultured on collagen-coated coverslips were fixed with 4% paraformaldehyde at 37°C for 15 minutes. After permeabilization and a blocking reaction, they were incubated with antibodies against N-terminal APC (H-290; Santa Cruz), C-terminal APC (C-20; Santa Cruz), α-tubulin (YL1/2; Abcam), paxillin (Abcam), and EB1 (Abcam). They were then treated with Alexa Fluor–conjugated secondary antibodies and phalloidin (Invitrogen), followed by staining with DAPI.

In Vitro Proliferation, Migration, Adhesion, and Tube Formation Assay

A BrdU incorporation assay was performed using the BrdU Labeling and Detection Kit III (Roch Diagnostics GmbH, Mannheim, Germany), according to the manufacturer protocol. Briefly, VECs were plated and labeled with 100 μmol/L BrdU for 6 hours. Cells were stained with the anti–BrdU-POD antibody and quantified by measuring absorbance with an enzyme-linked immunosorbent assay (ELISA) reader. The migration activity of VECs was measured using a wound healing assay, as described

previously.[22] Microscopic images were captured at 0 and 16 hours after culture, and the percentage of migrated area was quantified. The adhesion activity of the VECs was measured using a wash assay, as described previously.[23] For tube formation assay, the VECs were plated onto a layer of Matrigel (BD Biosciences, Franklin Lakes, NJ) and incubated at 37°C for 24 hours. Microphotographs of the formation of the capillary-like networks were obtained from at least four fields. Quantitative analyses of their tube length and the number of branching points were performed using WinROOF software version 6.0.

Plasmids

FLAG-tagged rat APC C-terminus (FLAG-APC-C-term), V5-tagged DLG1 and DLG5 plasmids were constructed. Briefly, the coding sequences of rat APC, DLG1, and DLG5 were amplified from brainstem cDNAs of F344/NSlc rats using KOD Plus Neo DNA polymerase (Toyobo, Osaka, Japan). APC C-terminus cDNA (321 amino acids) was cloned into the p3xFLAG-CMV-7.1 vector (Sigma). DLG1 and DLG5 cDNAs were cloned into the pcDNA6.2/V5/GW/D-TOPO vector using a TOPO Expression kit (Invitrogen). To increase efficiency of transfection, the truncated DLG5 cDNAs were cloned. The sequences of PCR primers to amplify the cDNAs are as follows: FLAG-APC-C-term, 5′-CATCTAGCGGCCGCCTCAAAGCGGCATGATATCG-CACGCTCCCATTCTG-3′ and 5′-CTTTCTGGATCCTT-TAAACAGACGTCACGAGGTAAGACCCAGAATGG-3′; DLG1-V5, 5′-CACCATGCCGGTCCGGAAGCAAGATA-CCCAGAGA-3′ and 5′-TAATTTTTCTTTTGCTGGGAC-CCAGATGTAAGGACC-3′; DLG5-V5, 5′-CACCATGGA-GCCGCAGCGCCGGGAGCTGCTCGCC-3′ and 5′-GGG-TGGGCAAGCGGGTATCCACAGGACTTT-3′; DLG5-1-V5, 5′-CACCATGGAGCCGCAGCGCCGGGAGCTGCT-CGCC-3′ and 5′-TTCCATTTGCTCCTTGAGTTCTTTA-3′; DLG5-2-V5, 5′-CACCTGTCAGCTGGAGAAGGAGGC-3′ and 5′-TGAGGTCTGAGGCTGGCTACAGAAG-3′; and DLG5-3-V5, 5′-CACCATGGGCTCTGACAGAGGCTCA-3′ and 5′-GGGTGGGCAAGCGGGTATCCACAGGACT-TT-3′. All constructs were verified by sequence analysis.

Co-Immunoprecipitation Assay

A co-immunoprecipitation assay was performed to examine binding reactivity of the C terminus of APC to DLG1 and DLG5. The recombinant V5-tagged rat DLG1 and DLG5 proteins were generated by human cervical cancer cells (Hela cells). Hela cells were cultured in Dulbecco's modified Eagle's medium (Life Technologies, Grand Island, NY) supplemented with 10% fetal bovine serum under an atmosphere of 95% oxygen and 5% carbon dioxide at 37°C. Hela cells were co-transfected with FLAG-APC-C-term plasmids and DLG1-V5, DLG5-V5, DLG5-1-V5, DLG5-2-V5, or DLG5-3-V5 plasmids using Lipofectamine LTX (Invitrogen). As a negative control, p3xFLAG-CMV-7.1 vector was used. The cells were lysed with Triton X-100 lysis buffer after incubation for 18 hours. The recombinant FLAG-APC-C-term proteins were purified and collected by immunoprecipitation using a FLAG Immunoprecipitation Kit (Sigma). As a positive control, FLAG-BAP fusion protein was used. The resulting supernatants were subjected to immunoblot analysis as described previously.[16] The primary antibodies were rabbit anti-EB1 monoclonal antibody (1:1000, Abcam), mouse anti-V5 monoclonal antibody (1:5000, Invitrogen), and mouse anti-FLAG M2 monoclonal antibody (1:5000, Sigma). The secondary antibodies were

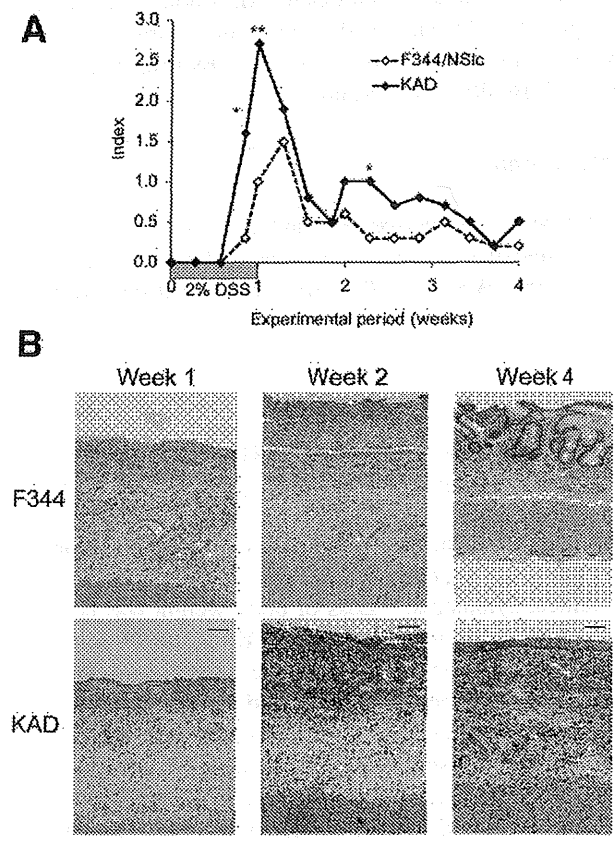

Figure 1 Sustained colon inflammation by DSS in the C terminus of APC-deficient rats. **A:** Clinical inflammatory scores for KAD and F344 rats that received 2% DSS in drinking water. The severity of inflammation was assessed by clinical scoring for diarrhea and fecal blood. $*P < 0.05$, $**P < 0.02$. **B:** Histologic sections of representative distal colonic lesions of F344 and KAD rats that received drinking water that contained 2% DSS. Pictures were obtained from F344 and KAD rats immediately after terminating DSS exposure (week 1), 1 week after terminating DSS exposure (week 2), and 3 weeks after terminating DSS treatment (week 4). Note mucosal denudation, crypts loss, and diffuse and marked infiltration of inflammatory cells, including polymorph neutrophils, plasma cells, and lymphocytes throughout the lamina propria and submucosa at weeks 1 and 2. At week 1, eosinophilic structures covering the damaged mucosa were observed for F344 but not for KAD rats. At week 4, the mucosal ulcer had healed by crypt degeneration accompanied by fibrosis and a diminished number of inflammatory cells in the F344 rats. However, mucosal ulcers accompanied by diffuse and marked inflammatory cell infiltrate, edema, and dilated small vessels were observed in the lamina propria and submucosa of the distal colon of KAD rats. In some KAD rats, elongation of squamous epithelium was seen on ulcerated mucosa. H&E staining. Original magnification ×200. Scale bar = 100 μm.

Table 1 Expression Levels of Inflammatory Cytokines in KAD Rats

	Week 0		Week 1		Week 2		Week 4	
Gene	KAD	F344/NSlc	KAD	F344/NSlc	KAD	F344/NSlc	KAD	F344/NSlc
Tnfα	1.26 ± 0.91	1.84 ± 1.53	0.47 ± 1.10	0.25 ± 0.30	88.93 ± 236.33	9.19 ± 11.50	3.24 ± 3.76*	0.22 ± 0.36
Il1β	0.24 ± 0.11	0.49 ± 0.32	118.08 ± 153.51	26.20 ± 33.14	927.33 ± 1204.49	889.79 ± 1233.85	110.61 ± 148.11*	4.70 ± 6.62
Il10	0.02 ± 0.01	0.04 ± 0.03	1.19 ± 1.59	0.26 ± 0.29	2.62 ± 4.37	3.17 ± 2.77	0.65 ± 0.77*	0.05 ± 0.05
Ptgs2/Cox2	0.75 ± 0.37	0.98 ± 0.18	0.34 ± 0.32	0.61 ± 0.77	186.45 ± 344.84	39.82 ± 101.57	13.66 ± 18.92*	0.16 ± 0.23
Ptges	0.62 ± 0.25	0.44 ± 0.46	13.14 ± 21.22	1.11 ± 1.56	73.20 ± 90.45	58.30 ± 77.77	11.49 ± 12.06*	2.18 ± 2.47

*$P < 0.05$.

horseradish peroxidase–conjugated anti-mouse and anti-rabbit IgG (1:2000, Sigma). Immunoblotted proteins were visualized using an ECL select Western blotting detection system (GE Healthcare, Piscataway, NJ).

Statistical Analysis

Student's *t*-test was performed, and SDs were calculated using the statistics package in Microsoft Excel (Microsoft Inc., Redmond, WA). $P < 0.05$ was considered statistically significant.

Results

KAD Rats Display Severe Acute Colitis and Sustained Colonic Inflammation

DSS can effectively induce colonic inflammation in rats, and a loss of body weight, diarrhea, and fecal blood are observed as the clinical symptoms.[24] Loss of body weight was noted from day 8 to day 10 in both F344 and KAD rats; however, there were no differences between the two strains of rat. There were no differences in water and food consumption during exposure to DSS (data not shown). KAD rats obtained higher inflammatory scores, mainly resulting from watery diarrhea and visible fecal blood, compared with F344 rats during exposure to DSS. This finding was true even after terminating exposure to DSS (Figure 1A).

Macroscopically, severe inflammation was generally located in the distal colon of the F344 and KAD rats. Prominent macroscopic features of KAD rat colon were dilation, primarily the distal part of the colon (one-third of the colon from the anus), thickening of the colonic wall, and extensive loss of the mucosa accompanied by bleeding. These findings were also observed in F344 rats, but the severity was less than that of KAD rats. The changes in KAD rats lasted until week 4; in F344 rats they lasted until week 2, and this was associated with their clinical symptoms.

Histopathologic analysis revealed the presence of mucosal ulceration, crypt loss, diffuse inflammatory cell infiltrate of the lamina propria and submucosa, debris, exudates, edema, and congestion and dilatation of the capillary blood vessels in the affected colons of both F344 and KAD rats at weeks 1 and 2 (Figure 1B). Of note, at week 1, eosinophilic structures covering the damaged mucosa were observed in F344 rats, whereas few structures

Table 2 Labeling Index Observed for DSS-Treated Colonic Mucosa

Week	F344	KAD
2	14.1 ± 7.9	16.1 ± 6.7
4	4.1 ± 1.5	8.5 ± 4.0*

The labeling index was calculated by dividing the number of BrdU-positive cells by the total number of nucleated cells per well-oriented crypt.
*$P < 0.001$ compared with F344 rats.

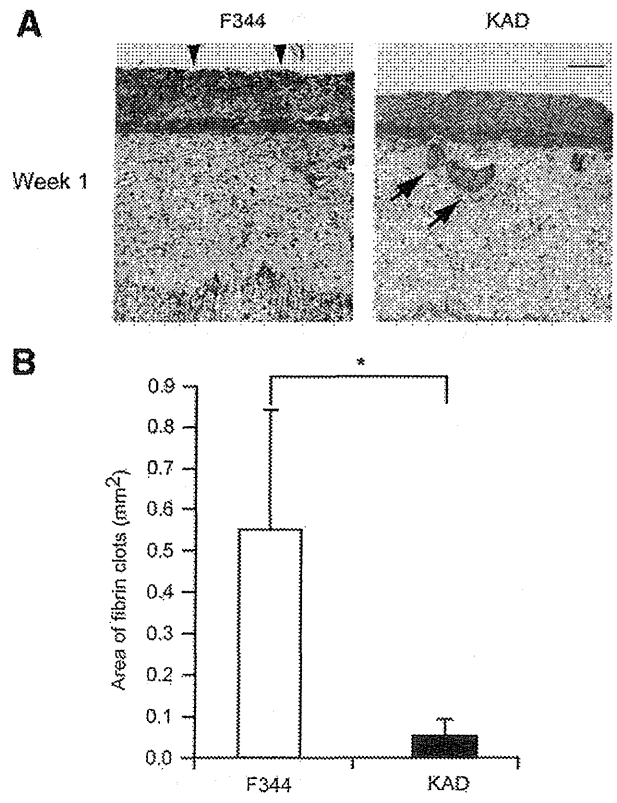

Figure 2 Lack of fibrin clot formation along the mucosal ulcer in the colon of KAD rats. **A:** PTAH-stained sections of F344 and KAD rats at week 1. Fibrin pseudo-membrane covering the surface of the damaged mucosal epithelia was observed in F344 rat colon (**arrowheads**). Fibrin pseudo-membranes were absent on the colonic mucosa of KAD rats; instead, fibrin microthrombi were observed beneath the lamina propria (**arrows**). Scale bar = 100 μm. **B:** The area of fibrin layers covering the surface of DSS-induced inflamed mucosa per rat. *$P < 0.001$.

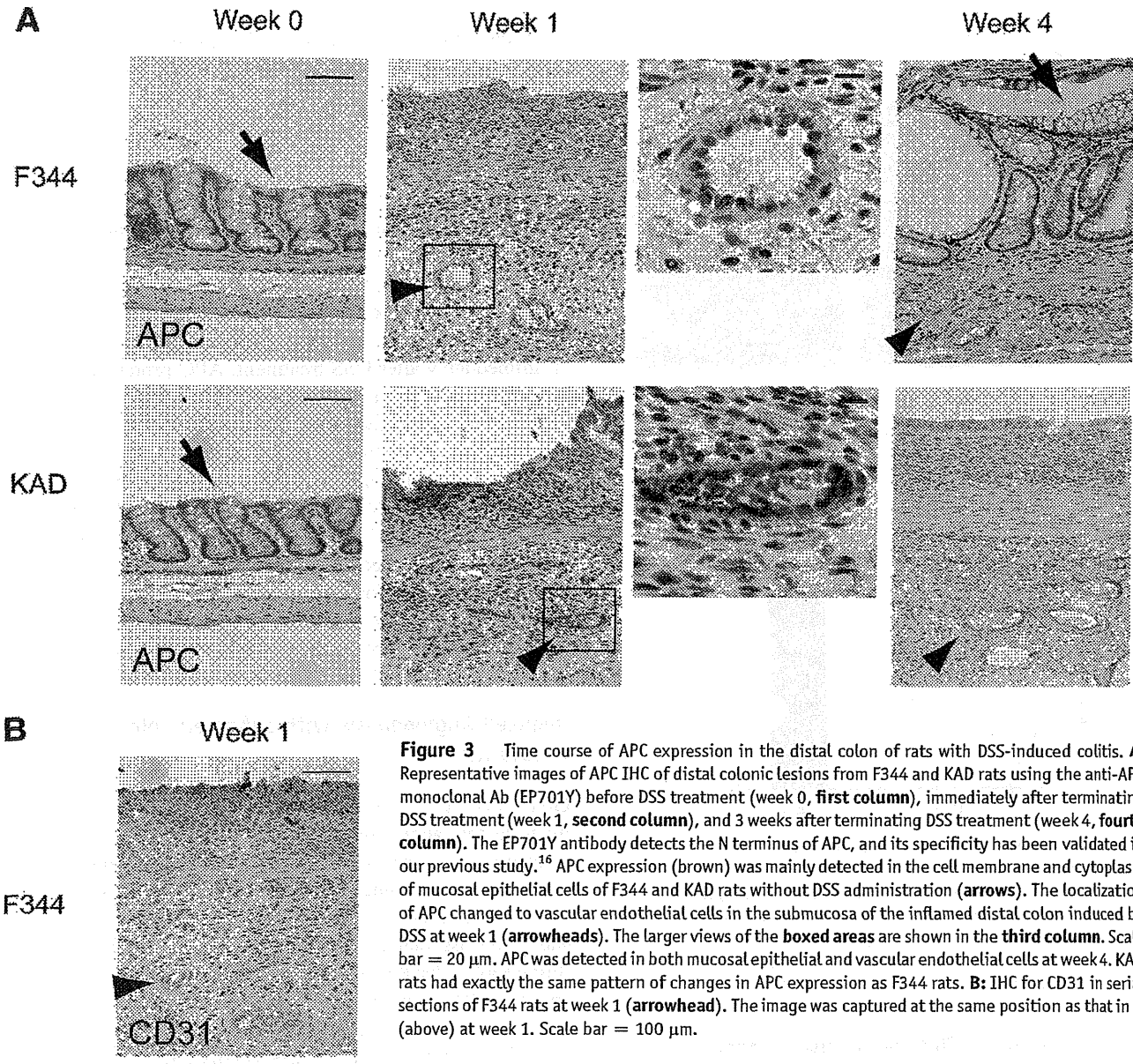

Figure 3 Time course of APC expression in the distal colon of rats with DSS-induced colitis. **A:** Representative images of APC IHC of distal colonic lesions from F344 and KAD rats using the anti-APC monoclonal Ab (EP701Y) before DSS treatment (week 0, **first column**), immediately after terminating DSS treatment (week 1, **second column**), and 3 weeks after terminating DSS treatment (week 4, **fourth column**). The EP701Y antibody detects the N terminus of APC, and its specificity has been validated in our previous study.[16] APC expression (brown) was mainly detected in the cell membrane and cytoplasm of mucosal epithelial cells of F344 and KAD rats without DSS administration (**arrows**). The localization of APC changed to vascular endothelial cells in the submucosa of the inflamed distal colon induced by DSS at week 1 (**arrowheads**). The larger views of the **boxed areas** are shown in the **third column**. Scale bar = 20 μm. APC was detected in both mucosal epithelial and vascular endothelial cells at week 4. KAD rats had exactly the same pattern of changes in APC expression as F344 rats. **B:** IHC for CD31 in serial sections of F344 rats at week 1 (**arrowhead**). The image was captured at the same position as that in **A** (above) at week 1. Scale bar = 100 μm.

were observed in KAD rats. Instead, eosinophilic deposits were observed under the lamina propria of KAD rats.

At week 4, the inflammatory changes and mucosal ulcers were resolved for F344 rats, healed by regenerative crypt cells associated with a reduction of the number of inflammatory cells. Severe inflammation was still present in the distal colon of KAD rats, and elongation of the squamous epithelium caused by squamous metaplasia was observed near the border between the rectum and anus. Immune cells, predominantly eosinophilic granulocytes, were continuously observed in the inflamed colon of KAD rats.

Consistent with the histopathologic observations, inflammatory cytokines and mediators, such as *Tnfα*, *Il1β*, *Ptgs2/Cox2*, and *Ptges*, and the anti-inflammatory cytokine *Il10* were expressed in the inflamed distal colon of DSS–treated KAD and F344 rats (Table 1). The cytokines were most highly expressed at week 2 in KAD and F344 rats. At week 4, the expression of those cytokines decreased in the DSS–treated F344 rat colons. In DSS–treated KAD rat colon, the expression of those cytokines was significantly higher than in F344 rats at week 4. These findings indicate that colitis in KAD rats was remarkably persistent even 3 weeks after termination of DSS treatment.

To assess cell proliferation in the mucosal epithelia, we measured the BrdU-labeling index for the colon epithelia. At week 1, few crypts were observed because of the disrupted architecture of the mucosa or ulceration. Thus, indices could not be calculated. At week 2, the indices were not different between KAD and F344 rats. At week 4, the index for the KAD rats was approximately half of that at week 2 but was significantly higher than that of the F344 rats (Table 2). These findings indicated greater persistence of cell proliferation in the KAD rats compared with the F344 rats at week 4.

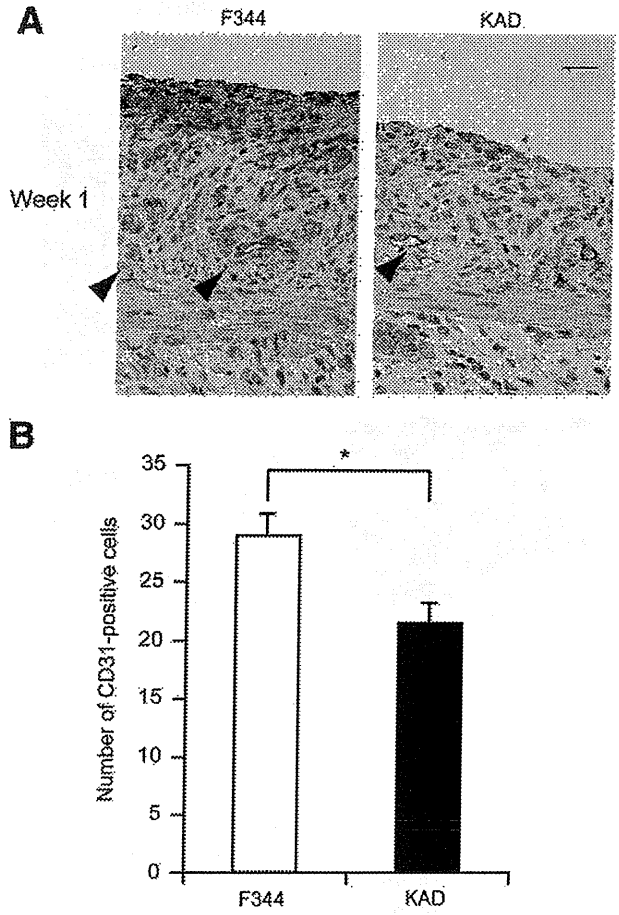

Figure 4 Reduction of angiogenesis associated with an absence of fibrin pseudo-membrane in the DSS-treated colon of KAD rats. **A:** IHC for CD31 of the distal colon of F344 and KAD rats at week 1. CD31-positive cells were clearly present along the ulcerated mucosa of F344 rats, whereas these cells were observed in much smaller numbers in the mucosa of KAD rats (**arrowheads**). Scale bar= 50 μm. **B:** Number of CD31-positive cells per field within the mucosa along the inflamed mucosa. $^*P < 0.001$.

The Absence of Fibrin Clots along the Damaged Mucosal Epithelia of KAD Rat Colon

To determine whether the eosinophilic structures that had been observed in the colon of F344 rats at week 1 were fibrin clots, we performed PTAH staining on the colonic tissue sections. For F344 rats, fibrin clots formed a pseudo-membrane covering the surface of the inflamed colonic mucosa (Figure 2A). In contrast, for KAD rats, formation of the pseudo-membrane consisting of fibrin clots was much less. Instead, fibrin was deposited mostly in microvessels immediately below the lamina propria and formed microthrombi. The area of the fibrin clots that covered the inflamed mucosa was significantly higher for F344 rats than for KAD rats (0.56 ± 0.29 mm^2 versus 0.057 ± 0.039 mm^2; $P < 0.001$) (Figure 2B). The area of fibrin microthrombi was significantly greater for KAD rats than for F344 rats (0.060 ± 0.048 mm^2 versus 0.0047 ± 0.0050 mm^2; $P < 0.04$). These results indicate that the formation of fibrin layers was defective over the damaged mucosa of KAD rats. Thus, the damaged mucosa of KAD rats has low potential to form fibrin layers, which make an important contribution to healing the eroded mucosa.

APC Is Expressed in the VECs in the Inflamed Colon

To find a potential association of the presence of APC with colitis, the expression of APC protein was examined in rat colonic tissue. Sequential change of APC expression was generally common in both F344 and KAD rats. At week 0, APC protein was expressed in the cell membrane and cytoplasm of normal mucosal epithelial cells (Figure 3A). At week 1, immediately after DSS treatment, APC protein was highly expressed in VECs in the inflamed submucosa, although no APC could be detected at the mucosal epithelial cells because of their disruption by severe ulceration. At week 4, the expression of APC had recovered in regenerative mucosal epithelial cells and VECs. We confirmed that APC-positive cells in the inflamed distal colon were VECs by immunostaining of serial sections using the anti-CD31 antibody, a positive marker for VECs (Figure 3B). These findings indicate that the expression of APC protein was induced in VECs of the submucosa when colon inflammation occurred.

Reduced Angiogenesis With Inflamed Colonic Mucosa in KAD Rats

Given that APC protein functions in VECs, we examined microvessel angiogenesis in the damaged mucosa by measuring the number of CD31-positive cells in the damaged colonic mucosa at week 1. For F344 rats, many CD31-positive cells were present along the mucosa, which was often associated with the presence of fibrin-like clots (Figure 4A). For KAD rats, fewer CD31-positive cells were observed. The number of microvessels per field along the inflamed mucosa of KAD rats was significantly lower than that of F344 rats (21.70 ± 1.59 versus 29.10 ± 1.83; $P < 0.001$) (Figure 4B). These results indicate that microvessel angiogenesis for healing was reduced in the damaged mucosa of KAD rats compared with F344 rats.

Truncated APC of KAD Rats Does Not Affect Wnt Signaling

To clarify whether a loss of the C terminus of APC could affect the regulation of Wnt signaling, we cultured REFs from E12.5 embryos of F344 and KAD rats. We then tested these REFs for their ability to inhibit Tcf-regulated transcription in transfection assays. TOPFLASH luciferase activity in the REFs from F344 and KAD rats was similar to control FOPFLASH activity. Luciferase activity in the REFs of both F344 and KAD rats increased with Wnt3a treatment (Supplemental Figure S1). These results indicate that truncated APC of KAD rats can normally regulate the Tcf-regulated transcription through a Wnt ligand.

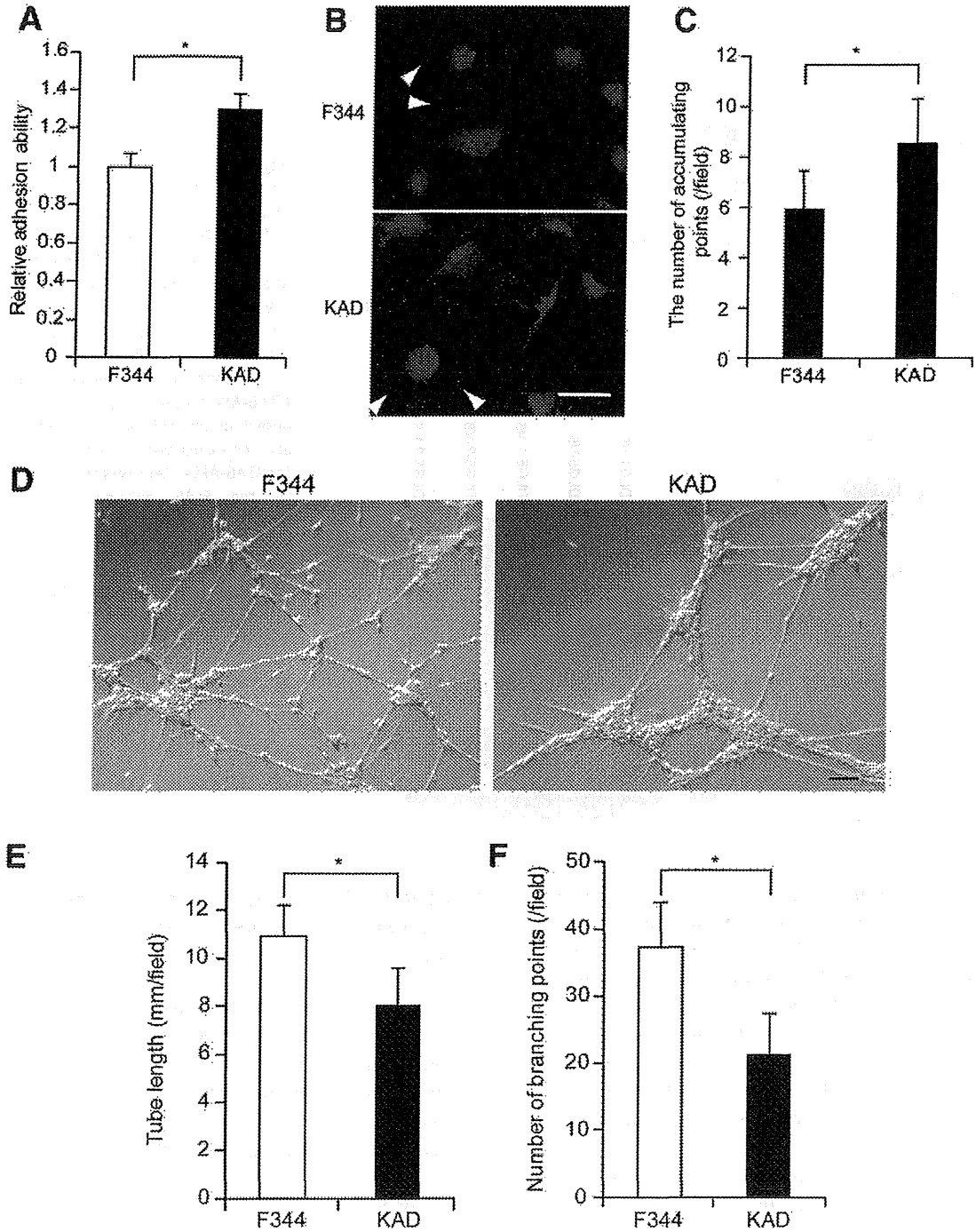

Figure 5 Involvement of APC in endothelial cell tube formation and adhesion. **A:** Wash assay for quantification of adhesion activity of F344 and KAD rat VECs incubated for 30 minutes on collagen-coated wells. Data ($n = 8$) are obtained from two independent experiments. *$P < 0.001$. **B:** Immunofluorescence of paxillin in F344 and KAD rat VECs. Accumulation of paxillin was observed around VECs (**arrowheads**). Scale bar = 50 μm. **C:** The number of paxillin-accumulating points as focal adhesions in five different areas at the cell periphery was counted in 20 cells. *$P < 0.001$. **D:** VECs isolated from F344 and KAD rats were plated onto Matrigel, and the formation of tube networks were photographed 24 hours after culture. Scale bar = 50 μm. **E** and **F:** Quantification of tubular length (**E**) and branching points (**F**) per field at ×100 magnification. Data ($n = 20$) are obtained from two independent experiments. *$P < 0.001$.

VECs of KAD Rats Show High Adhesion Activity and Abnormal Tube Formation

Migration, adhesion, and polarity of VECs play an essential role in angiogenesis, and their efficiency relies on dynamic rearrangement of the cytoskeleton.[25,26] To clarify the involvement of APC in angiogenesis, VECs were isolated from the thoracic aorta of F344 and KAD rats, and their physiologic functions were characterized.

KAD rat VECs had no apparent abnormal morphology when compared with F344 rat VECs and had no difference in the distribution or morphology of either MT or actin